Numerical Analysis of Combustion Dynamics for Coal Gasification

By

Bilal Hussain

School of Chemical and Materials Engineering (SCME)

National University of Sciences and Technology (NUST)

2018

Numerical Analysis of Combustion Dynamics for Coal Gasification

Bilal Hussain
00000119929

This work is submitted as a MS thesis in partial fulfilment of the requirement for the degree of

(M.S in Chemical Engineering)

Supervisor Name: Dr. Muhammad Ahsan

Co-Supervisor Name: Dr. Arshad Hussain

School of Chemical and Materials Engineering (SCME)
National University of Sciences and Technology (NUST),

April, 2018

Dedication

This thesis is dedicated to my parents

Abstract

During the combustion process of coal, the emissions pollute the environment. So, to control these emissions and to get the energy from coal the coal clean technologies are focused. The Integrated gasification clean coal is more efficient process and the numerical analysis play essential role in the improvement of gasification process. Different accepts of this process are analyzed. In this study the dynamic numerical approach is counseled to propose the fractions of different species present in the syngas produced during gasification because of volatile breakup. The volatile matter produced from solid fuel is composed of hydrogen, carbon, oxygen, nitrogen and sulfur. The composition of these species is estimated by species balance with their fraction existent in solid fuels. Computational fluid dynamic analysis is performed incorporating the volatile break-up predicted through finite volume method. Finite rate/Eddy dissipation model is implemented for reaction rates. The syngas outlet composition and temperature are examined with the experimental data. The analysis outcome that model results are within 10% precision with experimental data.

Keywords: Entrained flow gasifier; coal gasification; CFD; Finite rate/Eddy dissipation reaction model

Acknowledgments

Praise is due to **ALLAH** whose worth cannot be described by speakers, whose bounties cannot be counted by calculators, whom the height of intellectual courage cannot appreciate, and the diving's of understanding cannot reach; He for whose description no limit has been laid down, no eulogy exists, no time is ordained and no duration is fixed. Countless salutation upon **"HOLY PROPHET HAZRAT MUHAMMAD (S.A.W.W.)."**

I would like to acknowledge and express my sincere gratitude to my research **supervisor, Dr. Muhammad Ahsan** for his endless support, supervision and affectionate guidance to steer me in the right direction whenever she thought I needed it. I would also like to extend my gratitude to my research **co-supervisor, Dr. Arshad Hussain** and my Guidance committee members; **Dr. Sara Farrukh** and **Dr. Iftikhar Ahmad** for their valuable suggestions and guidance.

I would also like to thank **Dr. Arshad Hussain** (Principal, School of Chemical and Materials Engineering) and **Dr. M. Bilal Khan Niazi** (HOD, Department of Chemical Engineering) for providing a research-oriented platform to utilize my skills in accomplishing this research work effectively.

In the end, I must express my very profound gratitude to my parents for providing me with unfailing support and continuous encouragement throughout my years of study and through the process of researching and writing this thesis. This accomplishment would not have been possible without them.

Last but not least I would like to thank **Dr. Ammar Mushtaq** for being providing research facilities throughout my research project.

Bilal Hussain

Table of Contents

List of Figures

List of Tables

Chapter 1

Introduction

1.1 Background

Self-reliance in local energy resources is the reassurance for the country's economic development. In the light of recent fossil fuel consumption analysis, the most commonly explored oil and gas reserves will be exhausted in the subsequent half of this 21st century. Regarding the upcoming situation, to achieve self-sufficiency, substitute energy resources are being considered [1]. Conversion of solid coal into a gaseous fuel with high calorific value is widely accomplished today. In the 20 to 40 years of the last century, coal gasification was a common practice to produce manufactured gas in a number of plants around the whole world, and such plants were generally known as manufactured gas plants (MGPs) in those times [2]. This technology lost appeal after World War II era due to the ample resource and supply of petroleum and natural gas at reasonable prices. However, oil embargo enforced by Gulf oil producing countries in the early 1970s and following increases and instabilities in petroleum prices, as well as the shortage of natural gas and petroleum encountered in 2008-2009 when the whole world run into food and fuel crisis, the interest in coal gasification as well as its further commercial manipulation was invigorated [3].

Due to midterm exhaustion of oil and gas, coal gains significance not only as fuel providing cheap energy but also as feed for various industrial chemical syntheses. The available commercial gasification processes must be evaluated carefully for particular type coal feed to get best gasification yields [4]. The excessive ash, mineral and moisture content initially present in the coal feed are main challenges that arise in the coal gasification. The inclusive evaluation of gasification processes is challenging, as lots of governing variables such as coal structure and reactivity, temperature, pressure, steam requirement and other varying limiting conditions [2, 5].

1.2 Worldwide Coal Consumption and Production

Coal is the fastest-growing fuel in the last almost in every region of the world. Global production is greater than before by 6.1%. The Asia Pacific region is most prominent that is responsible for production growth of 85 % globally, led by China with 8.8 % increase the world's leading consumer and supplier. Coal consumption increased by 5.4 % with the Asia Pacific as the most prominent region in this net increase, while large regressions in North American consumption [6]. Coal has the prevalent Reserve/Production ratio among other conventional fuels. Europe & Eurasia has the largest regional reserves and has the highest R/P ratio, which shows they were not completely exploited. Coal consumption grew by 5.4% in 2011, the only hydrocarbon fuel to exceed the average growth and the fastest-growing form of energy other than renewable. Coal had a share of 30.3% of global energy consumption, the highest since 1969. Global coal production has increased by 6.1% with non-OECD countries accounting for nearly all of the growth. China is accounting for 69% of global growth [3, 6].

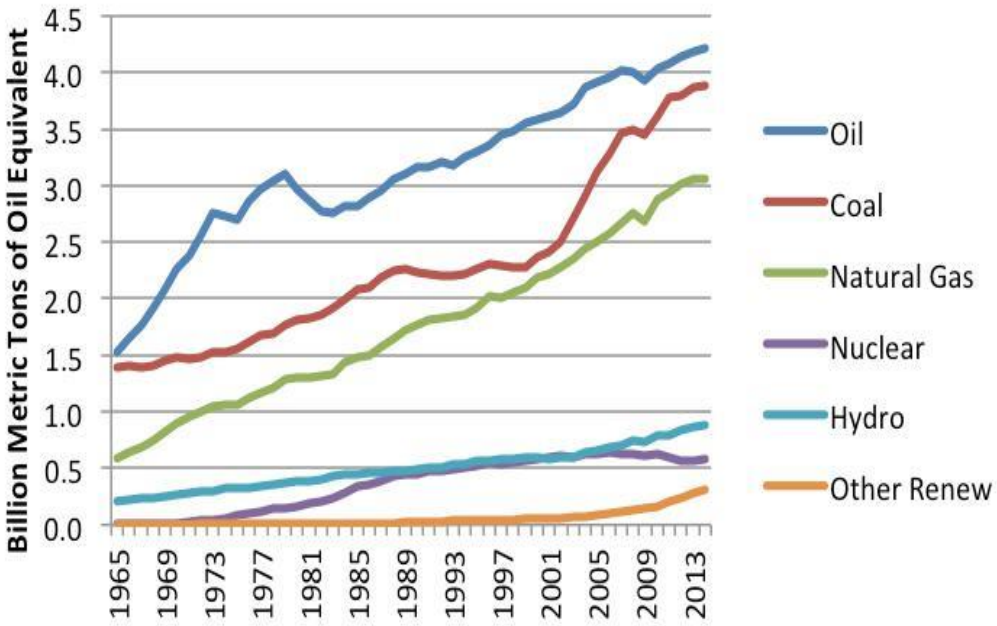

Figure 1 World's fuel consumption by source

1.3 Coal

The coal is fossil fuel which is present as sedimentary rock. Due to climate changes temperature and pressure the coal is form under the earth. It is composed of primarily of carbon, oxygen, hydrogen, nitrogen and has few traces sulfur and other compounds. Due to biological and geological changes during millions of years the dead plants and other organic compounds are converted from peat to anthracite with is considering have high-rank coal type. The conversion process from peat to coal is shown in figure (2).

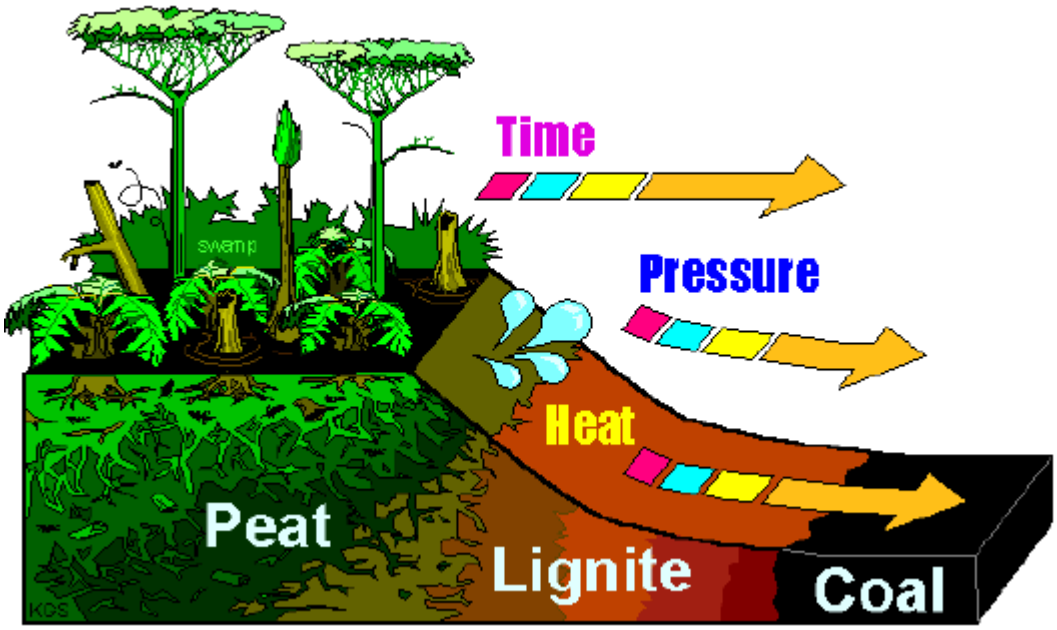

Figure 2 Coal Formation process

1.3.1 Rank of Coal

On the basis of carbon, hydrogen, oxygen, nitrogen, moisture content percentage presence the coal is divided into four ranks.

Lignite, Sub-bituminous coal, Bituminous coal, and anthracite are the types of coal on above basis. the lignite is considered as low-rank coal, and anthracite is known as high-rank coal.

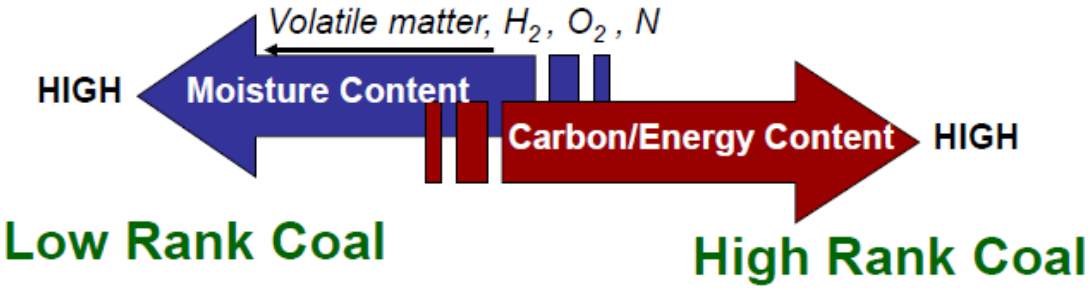

Figure 3 Coal Ranking

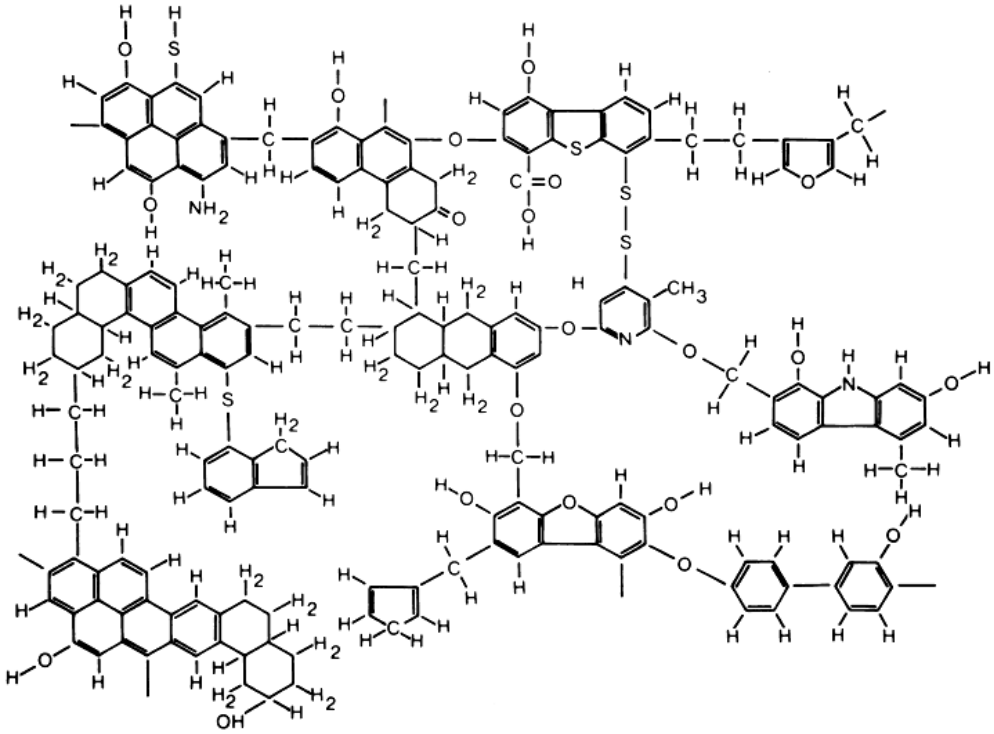

Figure 4 Coal Structure

1.4 Thesis Management

Chapter 1 describes the introduction. Gasification process, gasifiers used for gasification and literature review is discussed in chapter 2. Chapter 3 describes the Computational fluid dynamics-based modeling parameters, boundary and input parameters for gasifiers. Chapter 4 describes the results and discussion and in end conclusions, future recommendations are discussed.

Chapter 2

Literature Review

2.1 General Aspects of Gasification

For all the gasification reactions that take place, the conversion and reaction rate kinetics are typical functions of gas composition, nature and rank of coal, mineral content and moisture content of coal and operating variables like temperature and pressure. For a specific type of gasification reaction, the equilibrium of reaction shifts by either decreasing or increasing the temperature in all types of gasifier [7]. In general, the rate of reaction increases with small increase in temperature. However, in some particular reactions, the effect of pressure change cannot be ignored; it also affects the product gas formation [8, 9] Thermodynamics of carbon and hydrogen gasification reactions shows that methane production is enhanced at high pressures like 50 to70atm and temperatures ranging between (760-930^{o}C). In case of syngas production, at low pressure and high-temperature yield is maximum [10, 11]. Heat provision and heat recovery is an essential in gasification from the viewpoint of cost, design specification and operability. Char formed in pyrolysis is oxidized partially with steam leading to the generation of heat and synthesis gas. Through redox reaction of iron ore in a cyclic manner is an additional way to produce a synthesis gas stream associated with heat [7, 8] Downstream operations and further treatment of syngas depend on the rank of coal initially used in gasification. An Entrained flow gasifier on the hand is capable of handling almost any quality of coal feed, because the feed injection mechanism is different, forming a slurry or suspension of feed. However, if caking coals were gasified in a fixed bed or fluidized bed, some important changes are done, and special methods are employed to prevent caking. If cake formation or agglomeration happens in the gasifier, it seriously affects the normal operation of the gasifier in long runs [2].

Gas leaving contains sulfur in the form of sulfur dioxide, hydrogen disulfide or mercaptans, depending upon conditions and the nature of the reaction. Sulfur dioxide is produced if the oxidizing environment is there in the operation of gasification. The volatile matter (VM), fixed carbon content (FC), and the moisture content also plays an important part in coal treatment needs and processing in gasification [7, 12]. The

sulfur and nitrogen contents of coal determine whether post-treatment and waste heat removal requirements are significant. Sulfur may exist in three different types of coal. The pyritic sulfur and organic sulfur are more frequently found in coal whereas the sulfatic sulfur is present in oxidized or windswept then fresh coals [2].

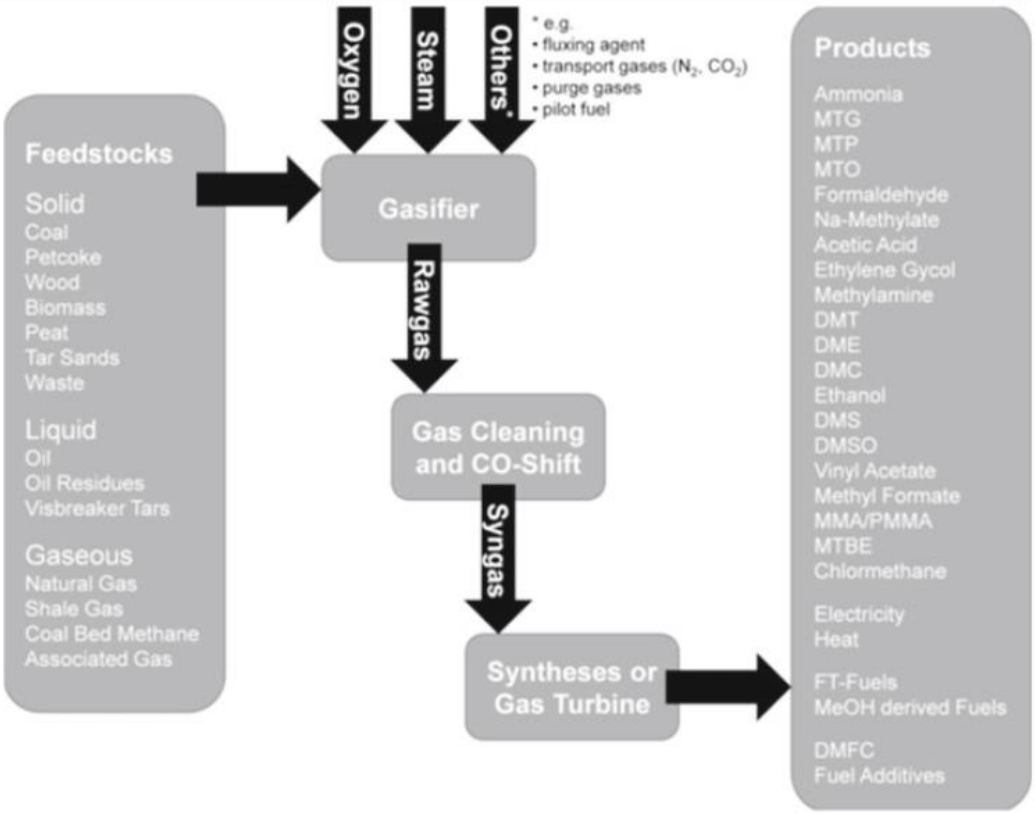

Figure 5 Overview of gasification feedstock and syngas utilization

2.2 Types of Gasifiers

- Fixed Bed Gasifier
- Fluidized Bed Gasifier
- Entrained flow Gasifier

2.2.1 Fixed Bed Gasifier

It is the oldest type of gasifier. For less power generation these gasifiers are suitable. These gasifiers are divided into different types on the bases of the direction of fuel and oxidant. These types are

- Updraft gasifier
- Downdraft gasifier

2.2.1.1 Updraft gasifier

The schematic diagram of this type of gasifier is shown in figure (6). The gasifying agent flows through the fixed carbonaceous fuel bed. The feed is entered form the top of the gasifier in the form of large particles and the gasifying agent is entered from the bottom of the gasifier. The feed started to move in a downward direction, and the gasifying agent is started to moving in an upward direction and in countercurrent flow the reaction takes place. That is why the updraft gasifier is also known as countercurrent gasifier.

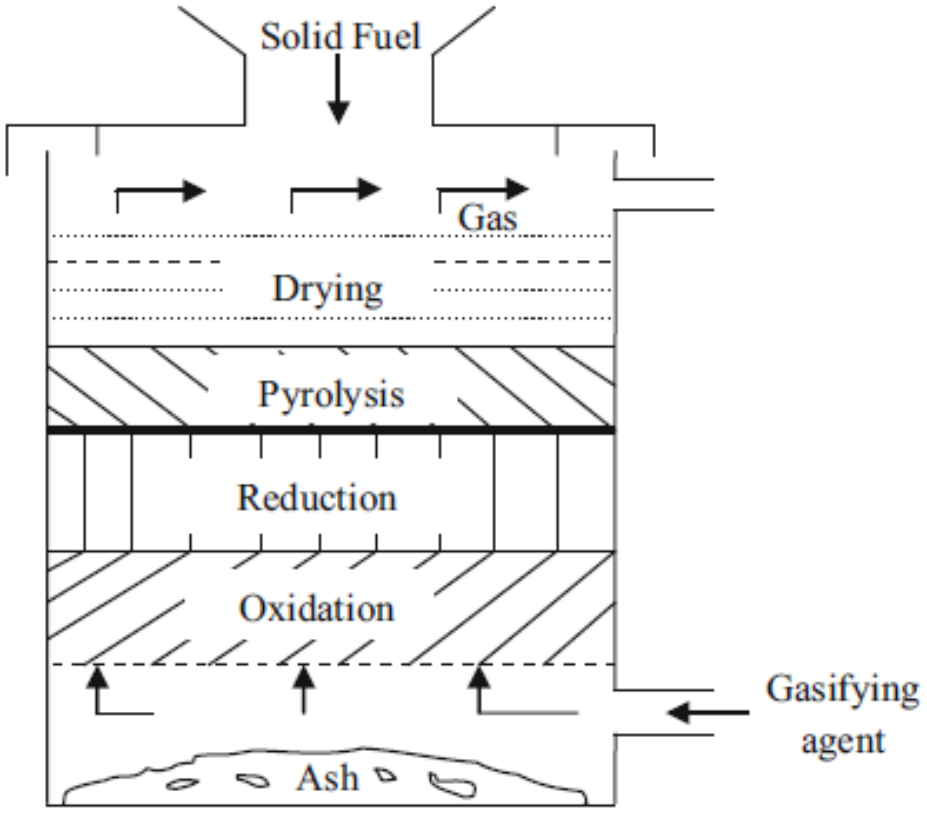

Figure 6 Updraft fixed bed gasifier

The moisture is removed from fuel in drying zone, and then fuel is entered into the pyrolysis zone where the volatile components are removed, and fuel is converted into char. The char is a move in a downward direction and enter into the gasification zone where the reduction is made after that in oxidation zone the char combustion is done by introducing the oxidizing agent [13].

The removal of ash in the form of liquid from the oxidation zone due to high temperature. The product gas produced from the gasifier is mostly from char

combustion and oxidation reactions. These gasifiers have relatively high thermal efficiency.

2.2.1.2 Downdraft Gasifier

Figure (7) show the schematic diagram of gasifier. The fuel is entered from the top, and the oxidizing agent is entered at the moderate level and the syngas is obtained at the bottom. These gasifier are also known as co-current gasifier because both fuel and oxidizing agent move in the same direction. The product gas produced in this gasifier have high outlet temperature.

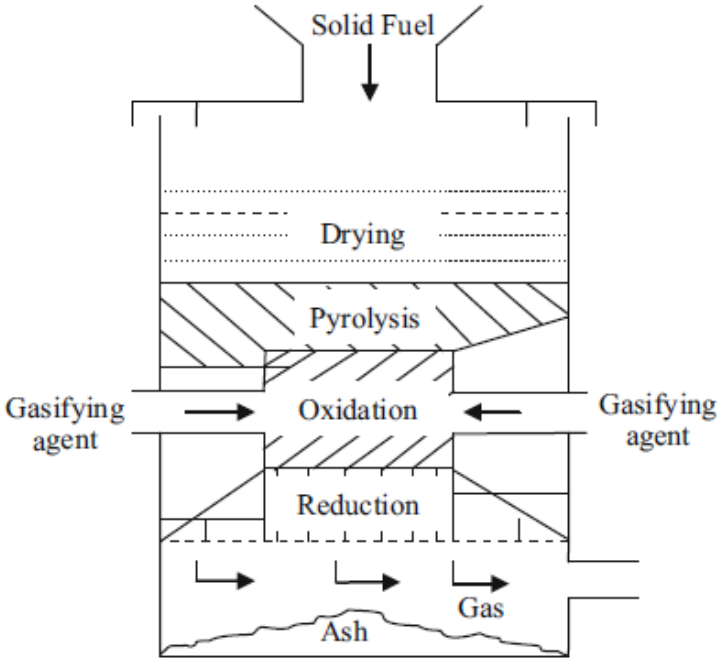

Figure 7 Downdraft fixed bed gasifier

The tar passes through the hot char keep in a downdraft and is converted into the gaseous product. From the top the solid fuel first enters into drying zone where it is dried by evaporating the water in the form of vapor. In the reduction zone, the some of the H_2O vapor reacts with char and form product gas. After the drying process, the fuel enters into the pyrolysis zone where the volatile matter and char are produced, and other products enter into oxidation zone where oxidation reactions occur by the introduction of an oxidizing agent.

2.2.2 Fluidized Bed Gasifiers

By the help of gas, the solid particles are converted into fluid form is known as fluidization. The feed used for the fluidized bed is in small particles, and from the

bottom of the reactor the fluidizing gases are entering to move in upward direction. In case of the fixed bed, there is defined a zone of drying, pyrolysis, reduction and oxidation zone but these are not defined in case of fluidized bed reactors. As there is no fixed zone in fluidized bed gasifier, so all the process of drying, pyrolysis, reduction- oxidation occurs in the whole gasifier that is why this is also known as the type of homogeneous reactors.

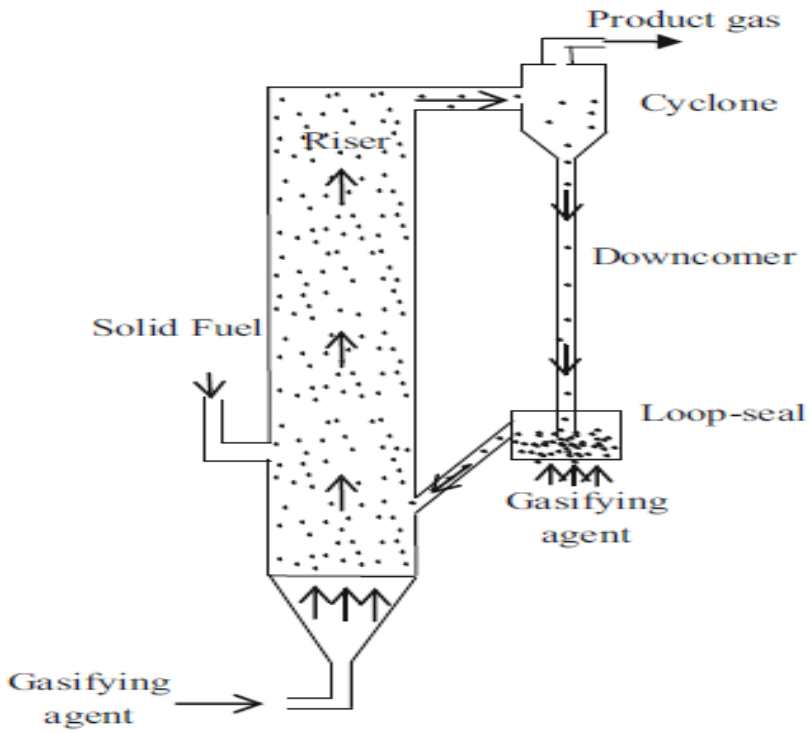

Figure 8 Fluidized bed gasifier

The gasifying agent in the fluidized bed gasifiers does two jobs the fluidization of particle bed and gasification of particles. In these gasifiers due to solid-gas excellent mixing, they have a controllable and uniform temperature, the conversation of carbon is high at a low tar production rate. Under different feed rate, feedstock, solid particle size and moisture content. These gasifiers have the flexibility to operate [14]. Due to increase in solid particles surface area, the reaction rate is increased in these reactors as compared to fixed bed reactors. Due to distinguishing features, the fluidized bed gasifiers scale up, and operation is easy as compared to fixed bed gasifiers. The residence time of these reactors are much less, but it can be increased by the continuous circulation of particles in circulating fluidized bed gasifiers. The coal and biomass both

can be used as feedstock in this type of gasifiers, but due to low gasification temperature of biomass, it is mostly used for biomass. In power generation (500kW to 50MW) set up these gasifiers are mostly.

2.2.3 Entrained flow gasifier

These gasifiers are mostly used the co-current flow of feedstock and gasifying agent. The schematic diagram of these gasifiers is shown in Figure (9). For these gasifiers both oxygen and air can be used as gasifying agent. The oxygen is used mostly in commercial gasifiers. The solid feedstock which has to enter in these gasifiers are much finer as compare to the particle size of solid particles which is used as feed in fluidized bed gasifiers.

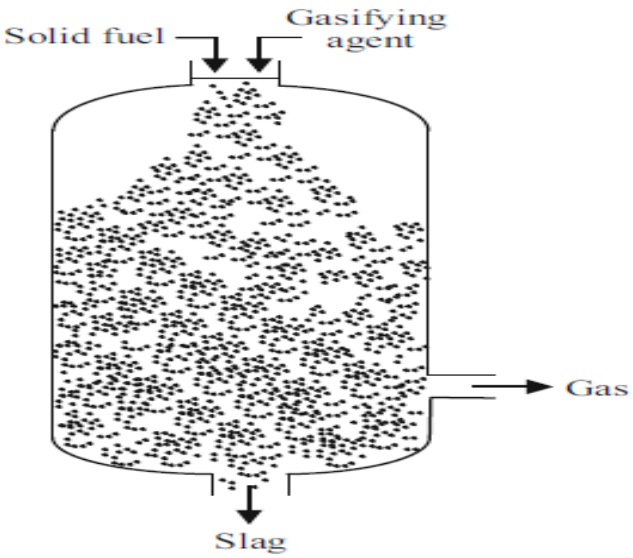

Figure 9 Entrained flow gasifier

As the fuel particle size is finer that means that surface area is increased and due to increase in the surface area of fuel particles when they entrained with a gasifying agent the reaction rate is increased and residence time is decreased. Due to this reason the operating temperature is increased and increase in temperature cause turbulence in flow which causes more conversation of fuel into product gas. The tar production in this type of gasifier is lesser due to a high operating temperature of gasifiers. These gasifiers can be used for any type of fuel feedstock. Whereas, the fuel with low moisture is best as a feedstock because it requires less amount of oxygen.

The fixed bed gasifiers are used for small-scale, fluidized bed gasifiers are used for medium scale, but the entrained flow gasifiers are mostly used for large-scale power

generation applications. The entrained flow gasifiers are mostly used for integrated gasification combined cycle coal power plants to produce several hundreds of MW.

The entrained flow gasifier is divided into different categories on the bases of following categories

2.2.3.1 Slurry feed and Dry feed

The commercially available gasifiers are operated at both dry and slurry feed. The gasifiers of MHI, Shell, Siemens, and PRENFLO are operated by using dry pulverized coal as feed whereas the GE, E-gas and ECUST gasifiers are operated by using the slurry coal as feed. The slurry coal is prepared by using rod mills through wet grinding [2]. Through the conveyers, the coal is sent into the rod mill feed inlet. Where coal is grinding into required particles size so that stable and optimum coal-water slurry is prepared. The use of slurry as feed has the disadvantage that loss of heat in the vaporization process of slurry and high concentration of oxygen is required for maintaining the required temperature of the gasifier. This problem leads to the low over the efficiency of the plant. Coal-water slurry is not feasible for low-rank coal because it already contains a considerable amount of inherent moisture.

Dry coal feeding is getting the great attraction for the low-rank coal which already contains significant moisture content. The lock hopper is used for the dry feed preparation. The operating pressure of lock hopper is low as compared to the coal-water slurry. Due to this, the thermal efficiency of the plant is decreased.

2.2.3.2 Oxygen-blown and air blown

The most of the commercial available entrained flow gasifier are oxygen blown. The air blown is MHI gasifier. The slurry feed system mostly operated with the oxygen-blown gasifier because of the remarkable sensible heat generation to evaporate the water from the slurry. The oxygen is used as oxidizing agent reduce the gasifier size and reduce the heat lost in the flue gas.

From the discussion of all types of gasifiers, the entrained flow gasifiers are seemed to be more feasible for the coal gasification and also can be used in large-scale power generation setup. By considering these points, the numerical simulation is based on this type of gasifier.

Table 1 Major Commercial entrained flow gasifier design

Manufacturer	Coal feeding	Oxidant	Flow-direction
SHELL	Dry	Oxygen	Upward
SIEMENS	Dry	Oxygen	Downward
PRENFLO PSG	Dry	Oxygen	Upward
PRENFLO PDQ	Dry	Oxygen	Downward
MHI	Dry	Air	Upward
HCERI	Dry	Oxygen	Upward
E-GAS	Slurry	Oxygen	Upward
GE (Texaco)	Slurry	Oxygen	Downward
MCSG	Slurry	Oxygen	Downward
Tsinghua OSEF	Slurry	Oxygen	Downward
ECUST	Slurry/Dry	Air/Oxygen	Downward

2.3 Literature Review

The generation of power is attainable from both renewable and non-renewable energy sources. However, the clean sources of power include the renewable resources like solar and wind energies as compared to non-renewable sources. The fossils fuels are also a non-renewable energy source. By using fossil fuels as a feedstock, technologies are being evolved for the inception of clean power. This is of high significance to deploy such systems which have the ability to produce eco-friendly outcomes and are economical as well [15, 16].

By deploying Coal as feedstock, the cleanest and efficient process considered for the generation of power is IGCC process [17, 18]. Through the process of gasification, the syngas and combustible gases are produced from coal or heavy hydrocarbons [19, 20].The gasification is the best suitable process to eliminate such gases which are responsible for the creation of corrosion. This process also enhances the production of convenient ignitable syngas [21].

For the gasification process fluidized bed, fixed and moving bed and entrained flow gasifier reactor can be used [16, 22]. However, In IGCC process, entrained flow gasifiers are used due to its high rate of utilization of carbon and their high reaction rate. Any type of coal can be used as feedstock and they operate at high temperature and pressure to produce tar-free syngas.

The Entrained flow gasifier can be updraft, downdraft and feedstock that is being used in it can be in dry or slurry form. Shell gasifier uses dry feedstock while E-gas gasifier

uses slurry feedstock. The E-gas type of entrained flow gasifier which is mostly used in IGCC is two stages, pressurized, updraft and oxygen is blown [23, 24].

CFD analysis is of high significance in designing and optimization of reactors because it proved the chemical conversion, thermal, hydrodynamics, operating parameters, coal quality effect on the mole fraction of syngas [25, 26].

In the oxygen-carbon dioxide blown gasifiers reactivity of char, gasification was observed in the presence of water and carbon monoxide, which result out that the presence of active sites of char improved the model accuracy [27].For the IGCC several modeling simulations are done [28, 29].All the researches are mostly based on mass balance, and thermodynamic analysis few of them are based on the steady state temperature to investigate the performance of gasifier [30, 31].Through the ASPEN model, the performance of gasifier ,the flexibility of use of feedstock , capital, and operating cost is investigated [22].By the simulation and numerical methods the steady state temperature and syngas composition is investigated [32-34].For the prediction of the temperature, reaction rate, product gas composition is investigated for the one dimensional entrained flow gasifier [34].

Many researchers developed different studies on gasifiers. Simulations are done to suggest optimum operating conditions and species comparison, concentration, and temperature with experimental data for pilot scale entrained flow gasifier [35]. For moving bed and fluidized bed, forecasting temperature changes and syngas production has been done, and systems are deployed to devolatilization for cracking model for it. For accurate prediction of syngas mole fraction in the gasifier, a simulation setup is developed based on Euler-Granular multiphase approach [36].

The effect on the performance of bubbling fluidized bed reactor due to the operating parameter is studied by both experimental and simulation [37]. In entrained flow gasifier, the controlling mechanism and turbulent mixing effect are studied for coal [38] . By changing operating parameters, the effect on gasification process is observed for two-stage entrained flow gasifier[39]. For entrained flow gasifier the turbulent particle dispersion and turbulence model sensitivity are explored [40]. For coal, the kinetic reaction parameters effect is explored for syngas composition in entrained flow gasifier [41]. The chemical and physical properties occur in gasifier and effect on gasifier performance is investigated at different conditions [42].

The species mole fraction and temperature changes are studied by using Illinios#6 coals as feedstock in E gasifier. Density/size effect of Pittsburgh coal on the product is investigated for E-gas [43]. The UDF is developed for devolatilization and improvement in evaporation for accurate numerical analysis of coal gasification [44]. Coal/oxygen ratio, slurry coal mass fraction feed rate of 1^{st} /2^{nd} stage for Illinois # 6 coal effect on E-gas gasifier performance. The O_2/Coal ratio decreases increases in Co and CO_2 and decreases in exit temperature [45]. Comparison of Illinois# 6 and North Dakota lignite coal particle size and cold gas efficiency effect on E-gas are observed and found out that it has high carbon conversion and is more efficient for coal particles having diameter 100 micrometers [45].

Chapter 3

Computational Fluid Dynamics Based Modeling

Computational fluid dynamics is a subdivision of fluid dynamics which uses data structure and numerical analysis to analyze and solve problems based on fluid flow. For the calculations, computers are required to simulate the gases and liquids interaction with surfaces described by boundary conditions. Better solutions can be achieved through high speed supercomputers. Many computational tools are developed through continuous research, which can enhance the speed and accuracy of complex simulation problems such as turbulent and transonic flows. This software is validated by experimental comparison using a wind tunnel, and final validations are done by flight tests.

3.1 Methodology

3.1.1 Preprocessing

The preprocessing consists of the following steps:

Computer Aided Design (CAD) can be used to define the physical bound and geometry of the problem. From there, fluid volume is extracted.

The volume which is occupied by the fluid is then divided into discrete cells (mesh). The mesh may be uniform or non-uniform, pyramidal or polyhedral, tetrahedral, structure or unstructured cells.

Now the physical mesh is defined using fluid motion, radiation, enthalpy and species conservation or non-conservation equations.

Boundary conditions are specified.

3.1.2 Processing

Simulations are processed until the convergence is reached and the set of equations are solved as steady-state or transient.

3.1.3 Post processing

Finally, the post-processing is done to aid the visualizing and analysis of the solution.

3.2 Simulation Environment

3.2.1 ANSYS Workbench

There are many geometries making software such as Gambit, Solid Works, Auto CAD, design modular, IGES, etc. Design modular is present in ANSYS workbench to others. So, Design modular is used to prepare geometry. In this work, three-dimensional geometry is prepared with the help of cylinders and cones. Cylinders and cones are connected with faces where required. After that geometry in imported into mesher where the Unstructured meshes are prepared and boundary conditions are labeled at edges while different zones are labeled at faces.

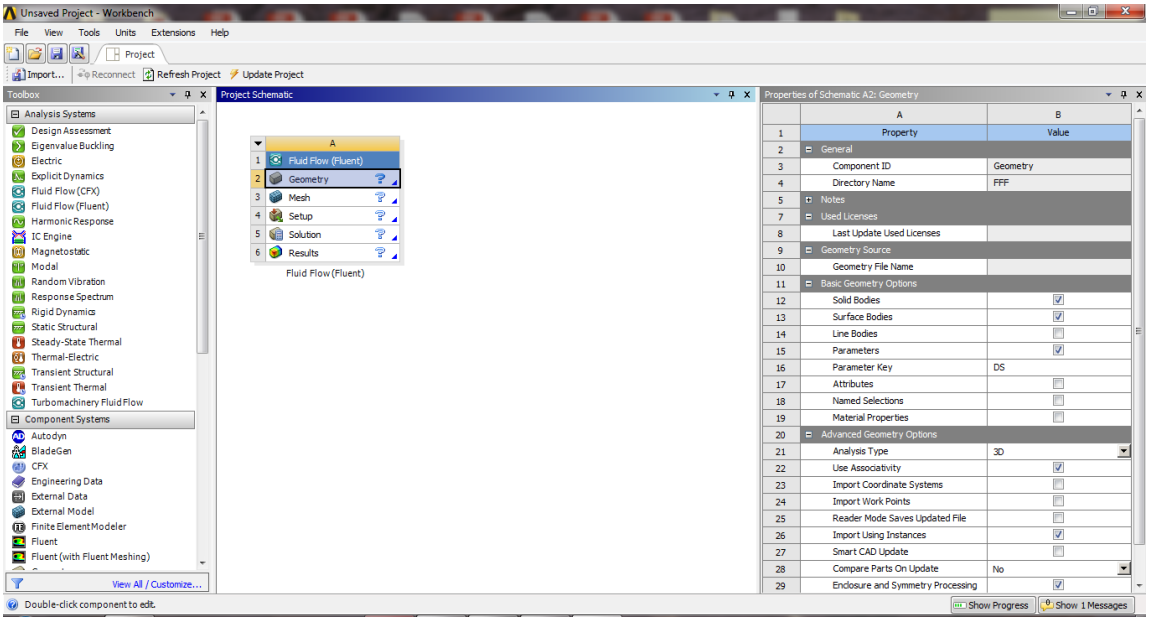

Figure 10 ANSYS workbench environment

3.2.2 ANSYS Fluent

Geometry is exported from design modular to the Fluent software which performs required simulation. Control volume method is used to solve the mass, energy, and species conservative equations. Mesh quality is calculated in ANSYS fluent. The boundary and zone conditions which are labeled in Design Modular software are now specified one by one in Fluent. Under solution method, pressure velocity coupling scheme is chosen and specified the spatial discretization for gradient, pressure, momentum, turbulent kinetic energy, turbulent dissipation rate, and species. Under solution control method, relaxation factors are adjusted for pressure, velocity, density, and other parameters. Residual monitors for absolute convergence are specified to find out the absolute convergence. After that initialization of solution is done and then

iteration is performed at different equations until the absolute convergence is achieved. Figure (11,12) shows the GUI of the ANSYS fluent tool.

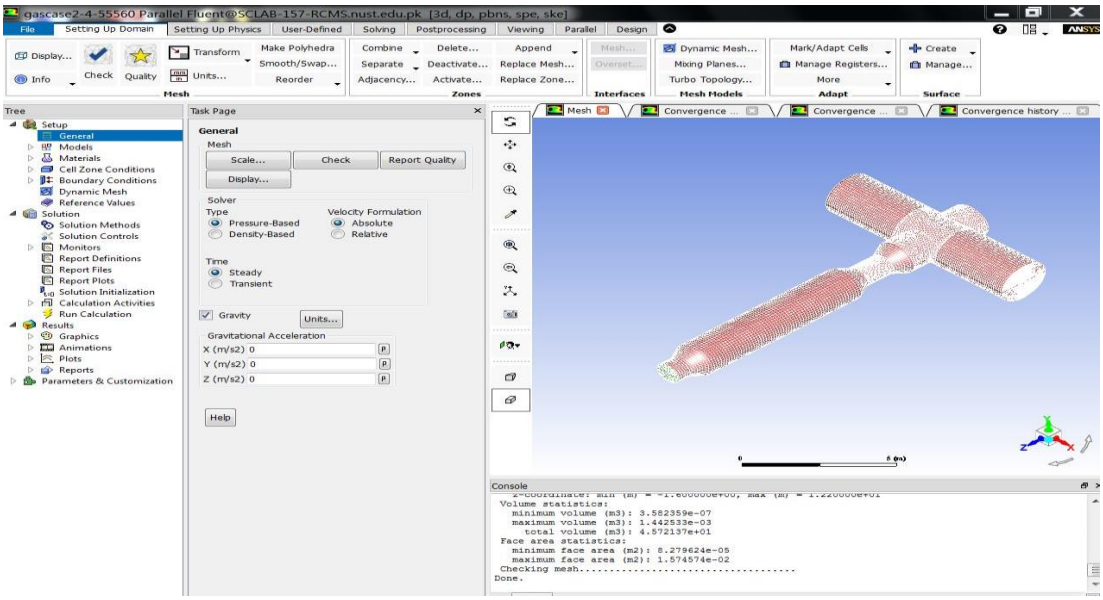

Figure 11 ANSYS Fluent Environment for E-gas

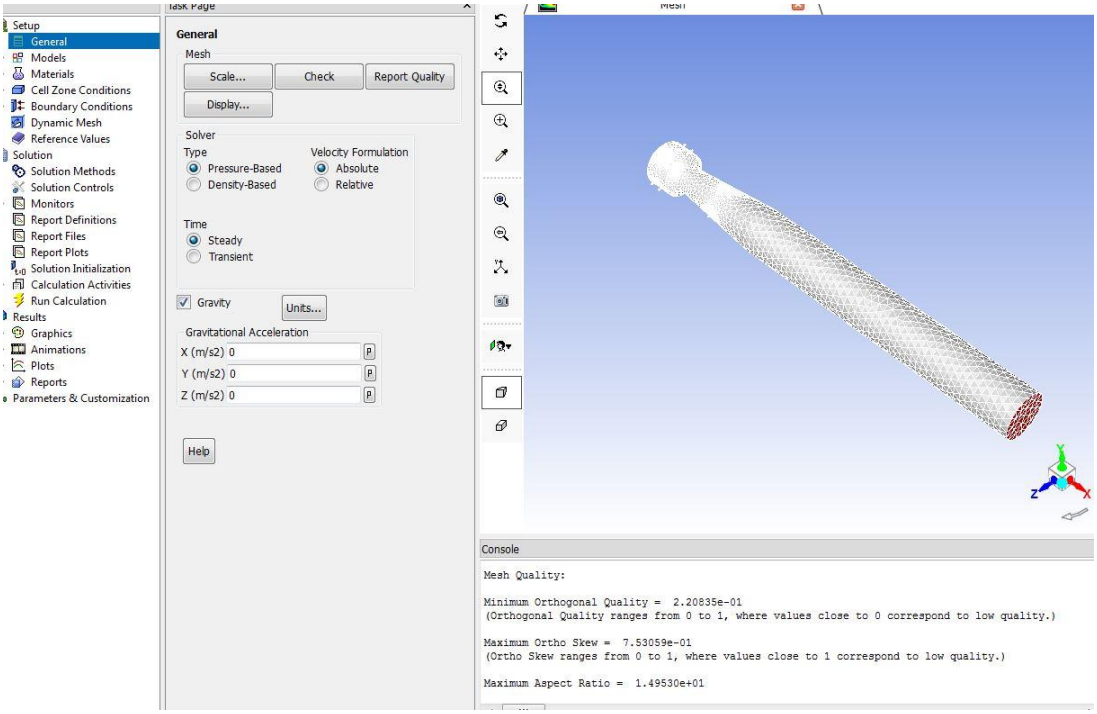

Figure 12 ANSYS Fluent Environment for air blown entrained flow gasifier

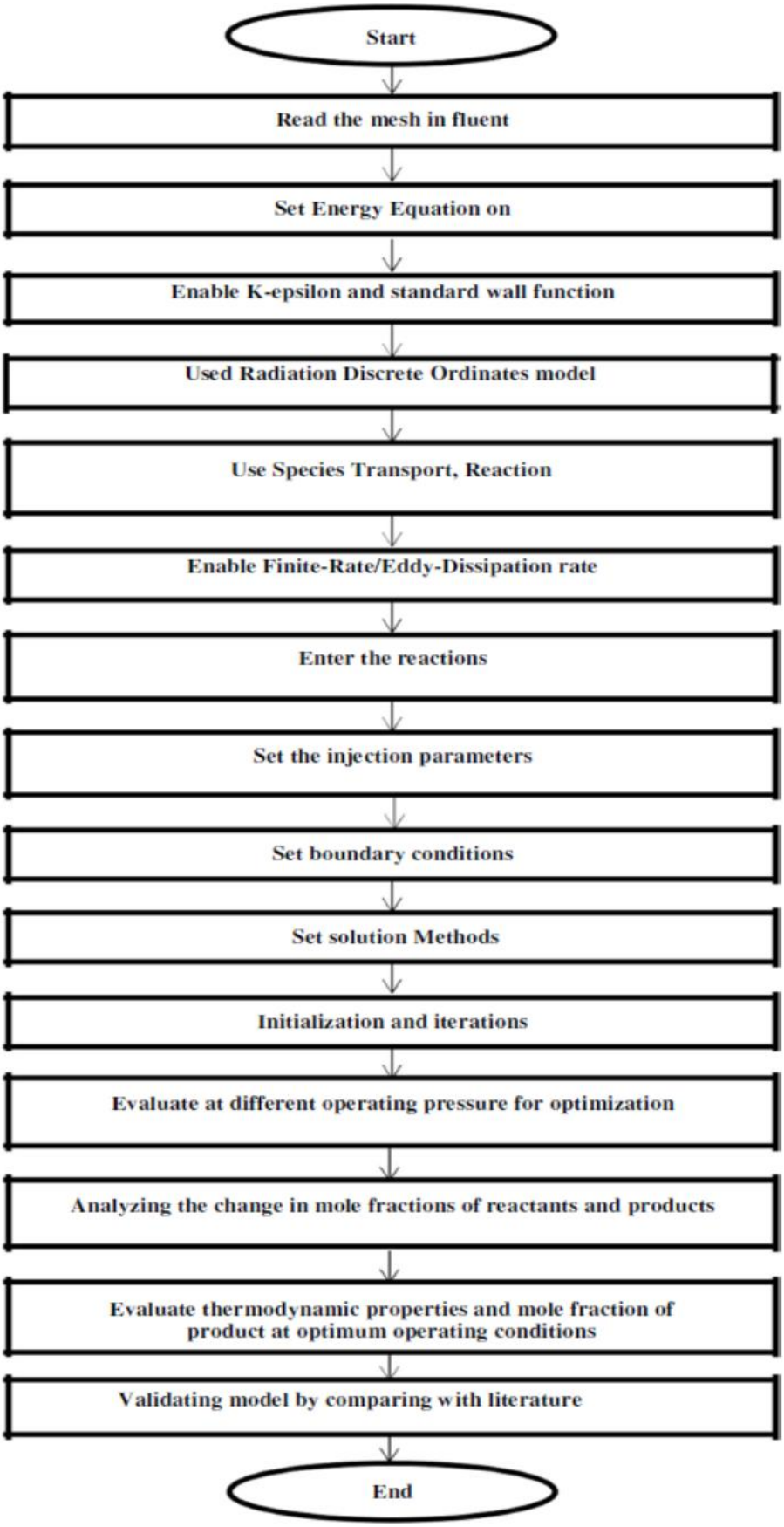

Figure 13 Schematic flow chart of the simulation setup

Thirteen reaction models; laminar finite-rate, finite-rate/eddy-dissipation rate, eddy-dissipation and eddy-dissipation concept are present in the fluent to deal with reactions and incorporate turbulence-chemistry interactions. In laminar finite-rate, Arrhenius expressions are used to calculate reaction rate and turbulence effects are ignored. In finite-rate/eddy-dissipation rate, both Arrhenius expression and mixing can influence the reaction. The smaller value of Arrhenius rate and mixing rate is considered the rate of reaction. In eddy-dissipation model, the reaction rate is controlled and determined by turbulence while in eddy dissipation concept model, Arrhenius expression is also incorporated in turbulent flames. Laminar finite-rate model is not recommended in turbulent conditions due to non-linearity in Arrhenius chemical kinetics. The values of different reaction parameters in these reaction models which includes a pre-exponential factor, activation energy, mixing law constants, stoichiometric coefficients and rate exponent are required to incorporate different reactions as shown in these figures.

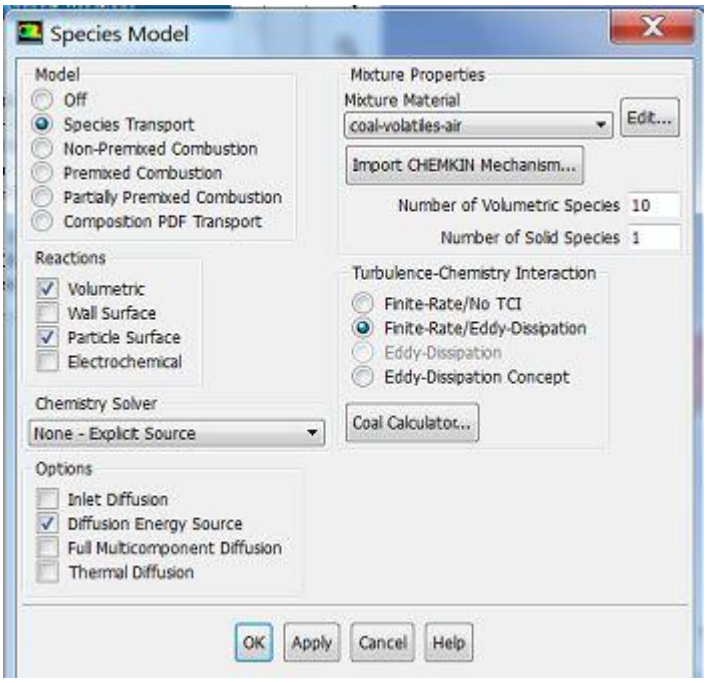

Figure 14 Species model

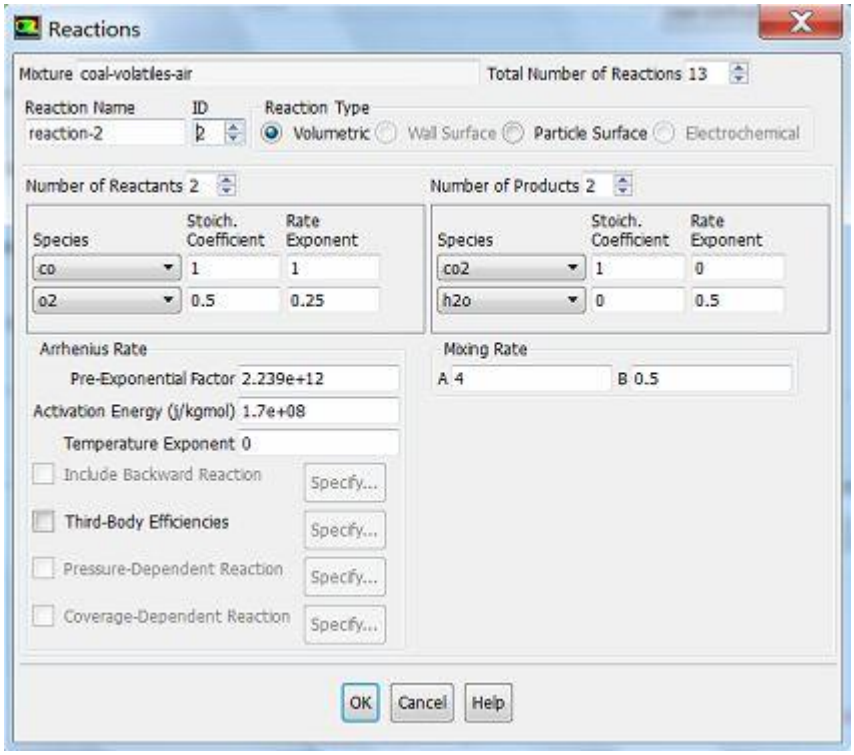

Figure 15 Reactions environment

3.2.3 Convergence criteria

The commonly used absolute convergence criteria for the residuals of continuity, x-velocity, y-velocity, epsilon and species equation is 0.001 while the convergence criteria are 1e-06 for energy equation. For the convergence, the absolute convergence criteria need to be satisfied.

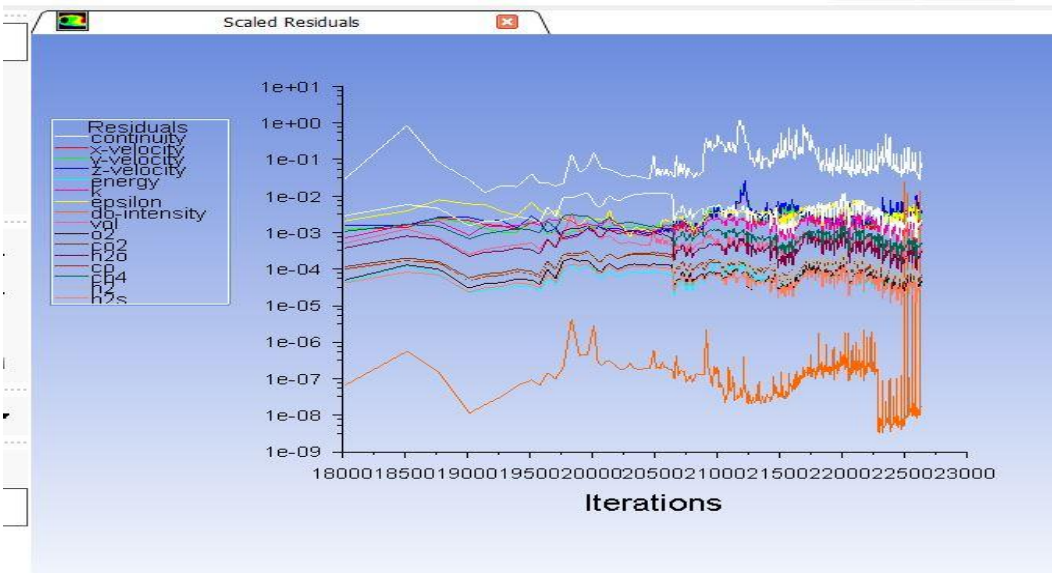

Figure 16 Scaled residuals

3.3 Geometry of all gasifiers

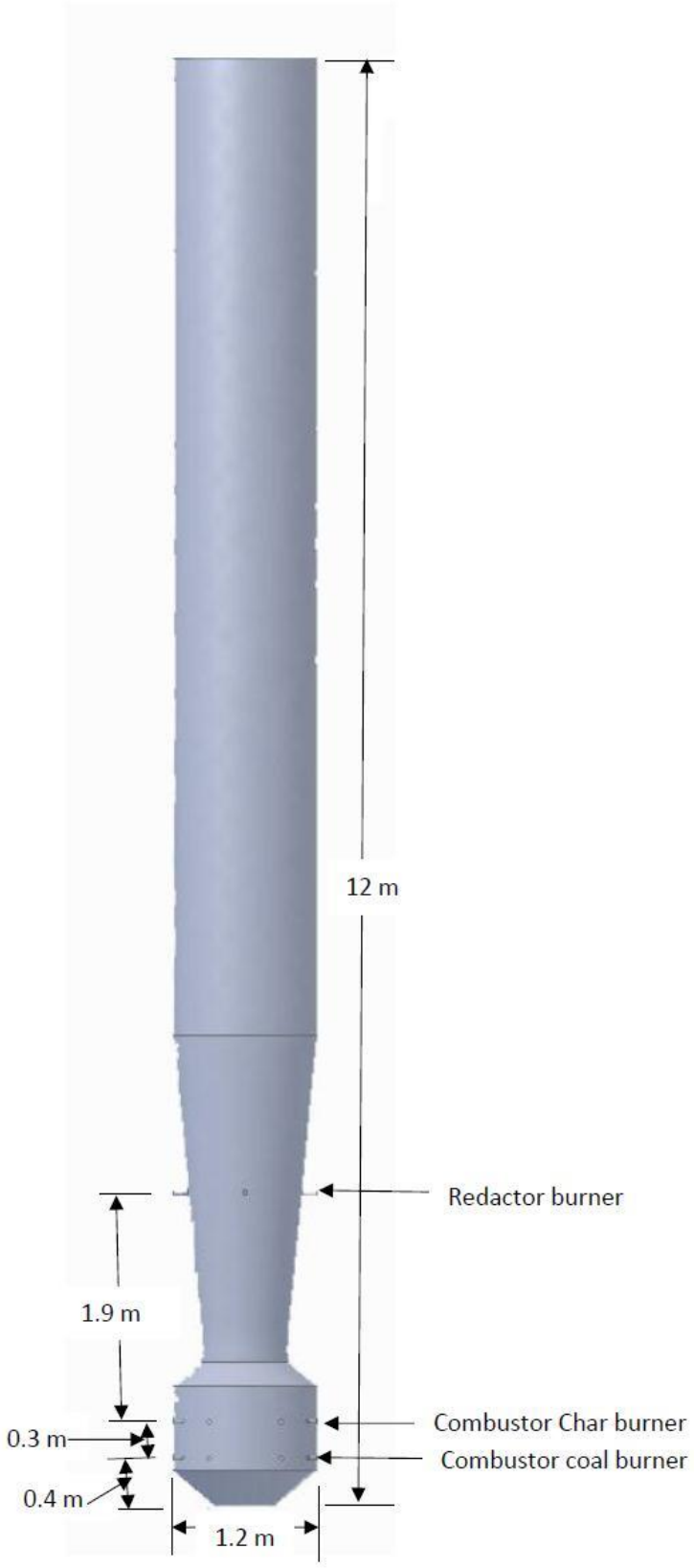

Figure 17 Geometry of air blown entrained flow gasifier

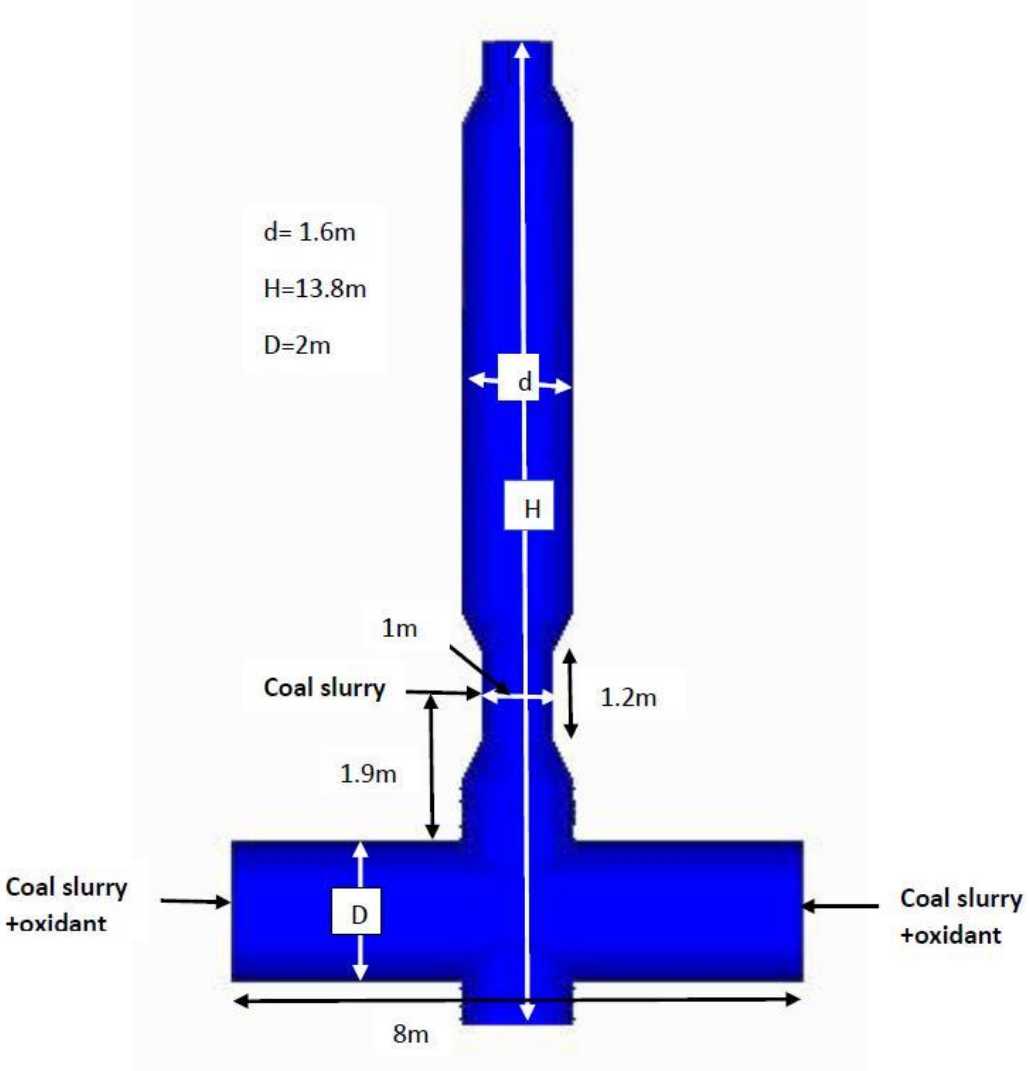

Figure 18 Geometry of E-gas entrained flow gasifier

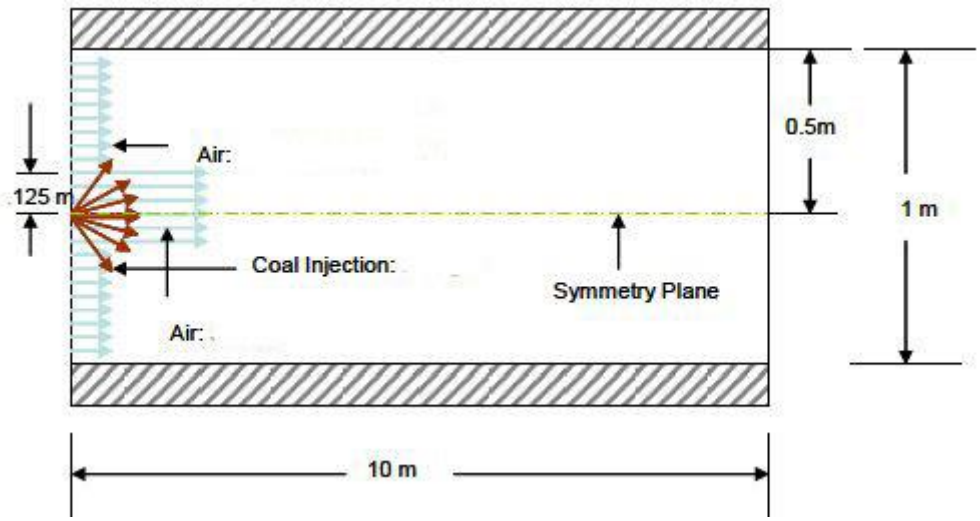

Figure 19 Geometry of Single stage gasifier

3.4 E-gas entrained flow gasifier

The entrained flow gasifier named E-gas is pressurized, up the flow, slurry feed, and two-stage gasifiers. The raw feed coal is converted into the slurry from wet crushers. The concentration of coal slurry is mostly in the range of 50 to 70% based on the inherent moisture and type of coal. The maximum coal slurry is introduced from the first stage of gasifier along with the oxidizing agent. Due to the high percentage of an oxidizing agent, the exothermic reactions are take place in the first stage. The exothermic reactions increase the pressure and temperature of 1st stage of the reactor due to which the hydrocarbons gases and liquid formation become negligible.

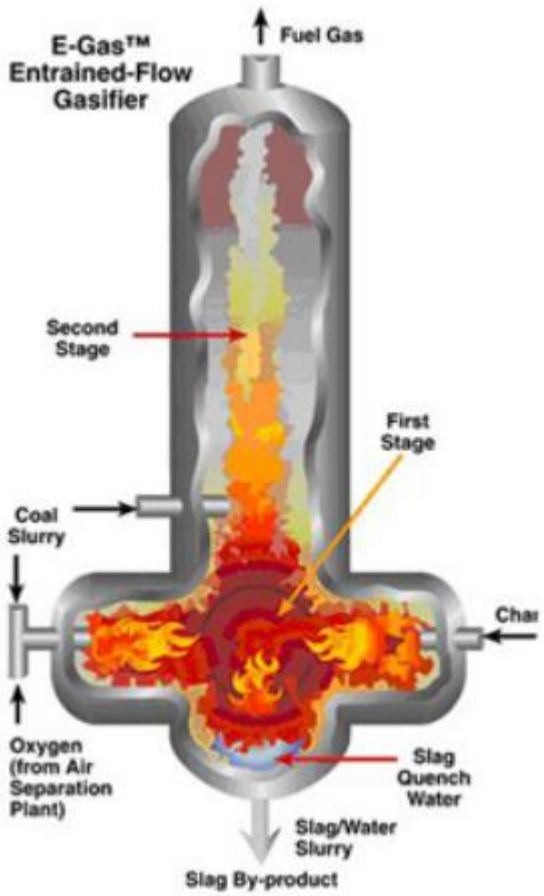

Figure 20 Schematic diagram of E-gas gasifier

The ash which is formed during the reactions is an exit from the bottom of the gasifier, and the quenching is done by the water. Due to quenching, it is converted into slag product. The product gases of the first stage are entered into the second stage of gasifier where almost 25% of slurry feed is introduced. Due to a limited oxidizing

agent in the second stage, the endothermic reactions and devolatilization reactions take place at 1310K.The hydrocarbon and char formation in this stage is recycled into the first stage. The syngas produced at 1310K is cooled by using the fir tube cooler where the steam is generated. In the wet scrubber, the chloride is removed from the syngas and char is recycled in the gasifier again. After that, the carbonyl sulfide and hydrogen sulfide removed from the syngas for the further applications of energy. The schematic diagram of the gasifier is as shown in figure (21).

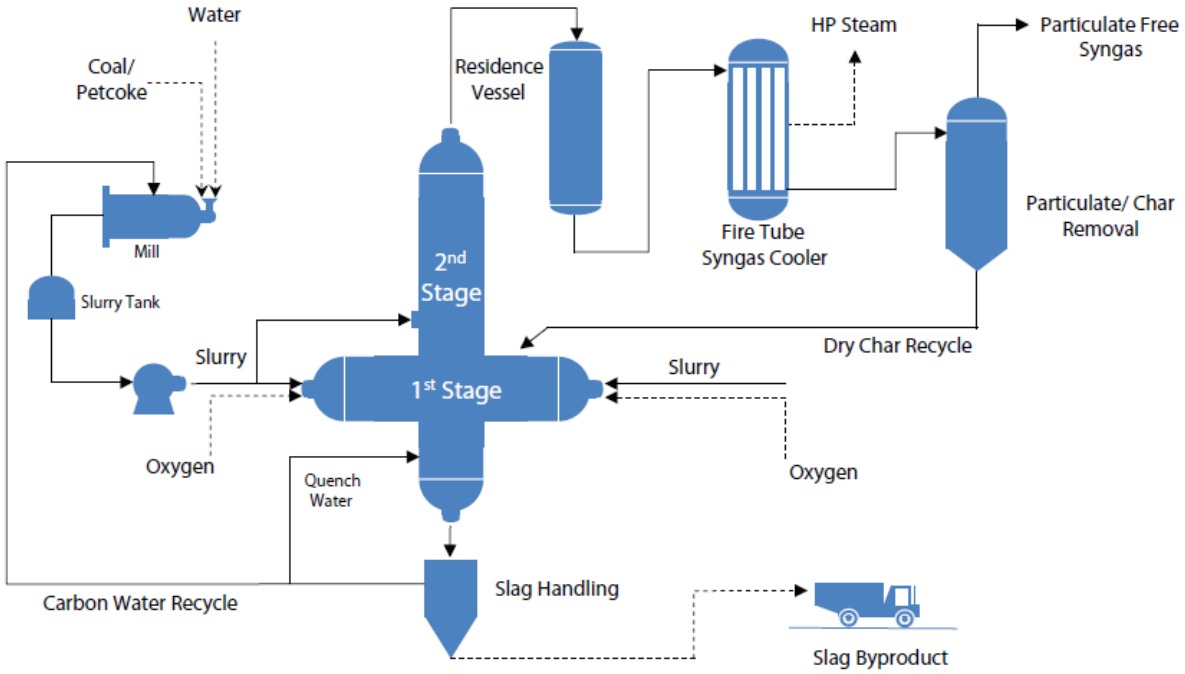

Figure 21 Process flow diagram of E-gas gasifier

3.4.1 Mesh and its properties

The geometry of both the gasifier is constructed in three dimensions. The three important parameters which give the quality of mesh are minimum orthogonal quality, maximum Ortho-Skew and maximum aspect ratio and their values are shown in the table. Figure (22) show the mesh of E-gas entrained flow gasifier and figure (24) show the mesh of air blown entrained flow gasifier. Table (2,5) presents the mesh characteristics for the E-gas and air-blown entrained flow gasifier respectively. The summation of all cells volume is equal to total volume of geometry.

Table 2 Mesh properties of E-gas

Properties of mesh E-gas	Values
Orthogonal quality(Minimum)	$2.4483e^{-1}$
Ortho skew (Maximum)	$7.21100e^{-1}$
Aspect ratio (Maximum)	$1.62576e^{+1}$
Minimum volume (m^3)	$3.582359e^{-7}$
Maximum volume (m^3)	$1.442533e^{-3}$
Total volume (m^3)	$4.572137e^{+1}$
Minimum face area (m^2)	$8.279624e^{-5}$
Maximum face area (m^2)	$1.574574e^{-2}$

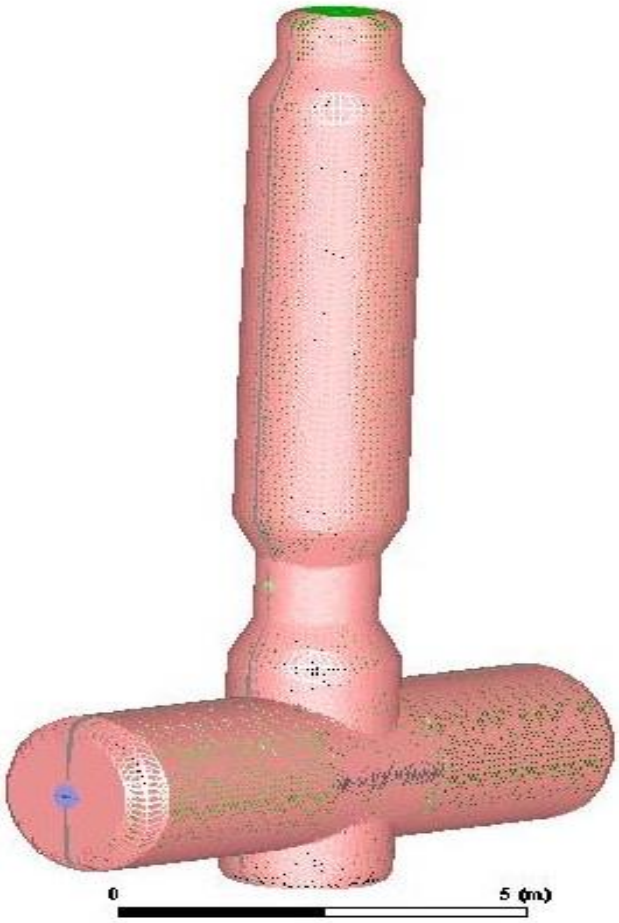

Figure 22 Mesh of E-gas gasifier

3.4.2 Boundary and Cell Zone Conditions for E-gas gasifier

The coal properties used in E-gas gasifier is given in table (3) and boundary conditions for gasifier are given in table (4) [46, 47] .

Table 3 Coal properties for E-gas gasifier

Proximate Analysis	Weight %
Fixed Carbon	54.65
Volatile	37.81
Moisture	0.3
Ash	7.22
Ultimate Analysis (DAF)	
Carbon	81.9
Hydrogen	5.61
Oxygen	8.86
Nitrogen	2.49
Sulfur	1.13
HHV	30.09MJ/Kg

Table 4 Boundary conditions

Operating and Boundary Parameters	Values
Operating Pressure	2.84 MPa
Inlet temperature	390 K
Oxygen mass fraction	0.944
First stage coal feed flow rate	10.84 kg/sec
First stage water feed flow rate	5.583 Kg/sec
Second stage coal feed flow rate	6.11 Kg/sec
Second stage water feed flow rate	3.15 kg/sec

3.5 Air Blown Entrained flow gasifier

The air blow entrained flow gasifier which is discussed here is MHI gasifier. It is dry feed, up the flow and two-stage operation reactors. The main focus on the air blown entrained flow gasifier is to use of it for IGCC applications.

The gasifier has three chambers the combustion, diffuser and the redactor zone. The combustion chamber is the lower zone. The dry mill is used to make the pulverized and dry coal which is injected from the inlets of combustion and the diffuser zone along with the oxidizing agent air. The exothermic reactions take place in the

combustion zone due to which the temperature of the combustion zone is increased. At the high temperature of the combustion zone, the coal ash is melt into the molten slag. From the bottom of the gasifier the molten slag is separated. The gases produced in the combustion zone is rising in an upward direction into the diffuser zone where more coal is added. The coal along with the product gases of combustion zone is a move into the redactor zone. Due to the endothermic reaction in the redactor zone its temperature is low as compared to the combustion zone. The syngas produced in the gasifier is an exit from the top of gasifier which is quenched by cooler by generating steam. The product gas which leaves the gasifier is at high temperature almost 2220^{o}F. So, the production of hydrocarbons gases and liquid is negligible. The schematic diagram of the gasifier is shown in figure (23).

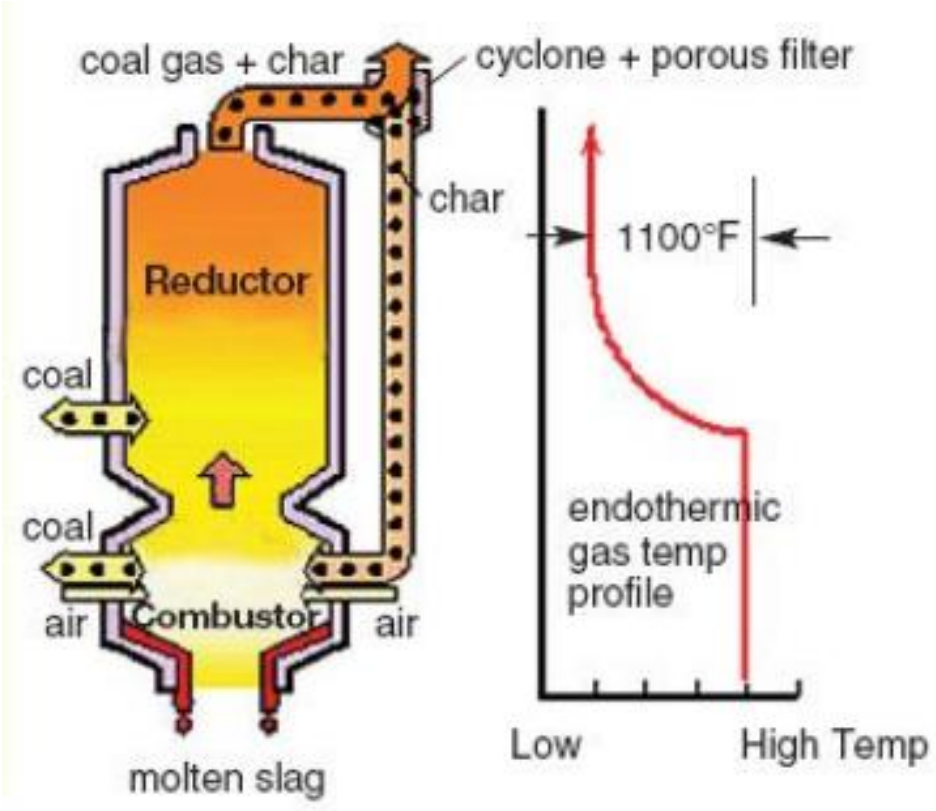

Figure 23 Schematic diagram of MHI gasifier

Table 5 Mesh properties of air blown entrained flow gasifier

Properties of mesh	Values
Orthogonal quality(Minimum)	$2.208e^{-1}$
Ortho skew (Maximum)	$7.53052e^{-1}$
Aspect ratio (Maximum)	$1.4953e^{+1}$
Minimum volume (m^3)	$2.754929e^{-8}$
Maximum volume (m^3)	$3.27359e^{-3}$
Total volume (m^3)	$1.207942e^{+1}$
Minimum face area (m^2)	$1.500644e^{-5}$
Maximum face area (m^2)	$4.85188e^{-2}$

Figure 24 Air-blown entrained flow gasifier mesh

3.5.1 Boundary and Cell Zone Conditions for air blown entrained flow gasifier

The coal properties used in air blown gasifier is given in table (6) and boundary conditions for gasifier are given in table (7) [32, 33].

Table 6 Coal Properties for air blown gasifier

Proximate Analysis	Weight %
Fixed Carbon	35.8
Volatile	46.8
Moisture	5.3
Ash	12.1
Ultimate Analysis (DAF)	
Carbon	78.25
Hydrogen	6.5
Oxygen	13.9
Nitrogen	1.13
Sulfur	0.22
HHV	2.7MJ/Kg

Table 7 Boundary conditions

Operating and Boundary Parameters	Values
Operating Pressure	2.7 MPa
Inlet temperature all levels	521 K
Air flow rate in combustion burner	4.708 kg/sec
Coal feed flow rate combustion burner	0.472 kg/sec
Air flow rate in char burner	4.708 kg/sec
Char feed flow rate char burner	1.112 Kg/sec
Air flow rate in reducer burner	1.832 Kg/sec
Coal feed flow rate reducer burner	1.832 kg/sec

3.6 Single Stage Gasifier

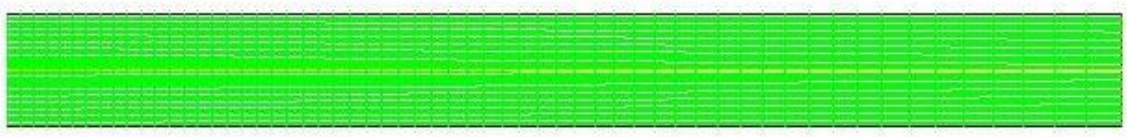

Figure 25 Mesh of single stage gasifier

3.6.1 Boundary and Cell Zone Conditions for single stage gasifier

The coal properties used in single stage gasifier is given in table (8) and boundary conditions for gasifier are given in table (9) [48].

Table 8 Coal properties for single stage gasifier

Proximate Analysis	Weight %
Fixed Carbon	50
Volatile	30
Moisture	10
Ash	10
Ultimate Analysis (DAF)	
Carbon	85
Hydrogen	10
Oxygen	4
Nitrogen	1
HHV	24.0MJ/Kg

Table 9 Boundary Conditions for single stage gasifier

Operating and Boundary Parameters	Values
Operating Pressure	2.7 MPa
Inlet temperature all levels	521 K
Oxygen Velocity inlet 1	25m/sec
Oxygen Velocity inlet 2	100m/sec
Coal feed flow rate	0.25 kg/sec

3.7 Numerical Scheme

The procedure for CFD of 3-D coal gasifier of E-type entrained flow gasifier, air blown entrained flow gasifier and 2-D simulation of single stage entrained flow gasifier is based on Navier-stokes equation which is computed by using Eulerian-Lagrangian approach. The coal particle is considered as discrete, and for this purpose, Discrete Phase model (DPM) is applied, DO radiation model, a k-ε model for turbulence flow. The operating parameters for the analysis are given in table (7,4)[33, 47]. The reaction involved in gasification are given in table 10. The reaction R2-R5 are heterogeneous surface reaction, and others are gas phase reactions.

3.7.1 Governing equations

Mass conservation equation is

$$\nabla.(\rho\overrightarrow{v}) = S_m \quad (1)$$

The water droplets vaporization and devolatilization of coal particles introduced from the dispersed second phase flow to the continuous phase.

. Conservation of momentum equation is:

$$\nabla.(\rho\vec{v}\vec{v}) = -\nabla p + \nabla.(\bar{\bar{\tau}}) + \rho\vec{g} + \vec{F} \quad (2)$$

Where static pressure, stress tensor is denoted by p and τ ρg and F show the gravitational and external body forces. That arises from the dispersed phase interaction respectively

The stress tensor τ is given by

$$\bar{\bar{\tau}} = \mu[\left(\nabla\vec{v} + \nabla\overrightarrow{v^T}\right) - \frac{2}{3}\nabla.\vec{v}I \quad (3)$$

Where molecular viscosity is μ, *I* is the unit tensor,

The conservation of energy is:

$$\frac{\partial}{\partial x_i}(\rho\overline{u_i}h) = \frac{\partial}{\partial x_i}\left(K\frac{\partial T}{\partial x_i}\right) + S_{ph} \quad (4)$$

3.7.2Turbulence Model

The turbulence model is based on kinetic energy k, and dissipation rate ε are computed by using k-ε transport equations (5,6). The turbulence kinetic energy generation Gk because of velocity gradients. The turbulent Prandtl number for k and ε are σ_k , σ_ε respectively. From equation (7) the eddy viscosity is calculated.

$$\frac{\partial}{\partial x_i}(\rho k u_i) = \frac{\partial}{\partial x_j}\left[\left(\mu + \frac{\mu_t}{\sigma_k}\right)\frac{\partial k}{\partial x_j}\right] + G_k - \rho\varepsilon \quad (5)$$

And

$$\frac{\partial}{\partial x_i}(\rho\varepsilon u_i) = \frac{\partial}{\partial x_j}\left[\left(\mu + \frac{\mu_t}{\sigma_\varepsilon}\right)\frac{\partial \varepsilon}{\partial x_j}\right] + C_{1\varepsilon}\frac{\varepsilon}{k}G_k - C_{2\varepsilon}\rho\frac{\varepsilon^2}{k} \quad (6)$$

$$\mu_t = \rho C_\mu \frac{k^2}{\varepsilon} \quad (7)$$

The empirical model constants used in above equations are $C_{1\varepsilon} = 1.44$, $C_{2\varepsilon} = 1.92, C_\mu = 0.09, \sigma_\varepsilon = 1.3, \sigma_k = 1.0$ [45].

3.7.3 Devolatilization

The coal particles devolatilization reaction are computed by using two rate models. The constants values are A_1 = 2×105, A_2 = 1.3×107, E_1 = 1.046×108 J/kg mol, and E_2 = 1.67×108 J/kg mol.

$$R_1 = A_1 e^{-(E_1/RT_p)} \quad (8)$$

$$R_2 = A_2 e^{-(E_2/RT_p)} \quad (9)$$

Weight function for devolatilization based on the kinetic rates which are obtained from equation (8,9). The yield factors are α_1 and α_2; moisture mass fraction is f_ω, particle mass and ash mass are m_p, ma respectively are the parameters used in equation (10)

$$\frac{m_v(t)}{(1-f_{\omega,0})m_{p,0}-m_a} = \int_0^t (\alpha_1 R_1 + \alpha_2 R_2)\, exp\left(-\int_0^t (R_1 + R_2)\, dt\right) dt \quad (10)$$

The heterogeneous reaction is based on the particle surface, and the depletion rate of carbon because of surface reactions are based on relations given in equation (11,12,13) [45] .In gas phase particle yield endothermic reaction and the reaction rate $\widetilde{R_k}$ (kg/sec) for depletion of particle surface are calculated from equation (8).The parameters used in these relations are particle surface area A_p ,effectiveness factor η_k, mass faction for particle surface species p_i .diffusion rate coefficient D_k, reaction kinetic rate k_{kin} and apparent reaction order N_k.

$$\overline{R_k} = A_p \eta_k Y_{carbon} \widetilde{R_k} \quad (11)$$

$$\widetilde{R_k} = k_{kin,k}\left(p_{i,k} - \frac{\widetilde{R_k}}{D_k}\right)^{N_k} \quad (12)$$

$$k_{kin} = A_f exp^{-(E_\infty/RT_p)} \quad (13)$$

The water which is present in coal slurry particle is considered as small droplets, and the rate of vaporization of water is controlled by the surface and gas streams difference concentrations. The rate of change of droplet mass is given in equation (14). The mass transfer coefficient k_c calculated by empirical correlation of equation (15) relative Reynolds number Re_d depends on relative velocity and particle diameter, vapor concentration at particle surface C_S calculated by using assumption of flow over the saturated surface, bulk flow vapor concentration C_∞ are parameters used for droplet mass gradient.

$$\frac{dm_p}{dt} = \pi d^2 k_c (C_s - C_\infty) \quad (14)$$

$$Sh_d = \frac{k_c d}{D} = 2.0 + 0.6 Re_d^{0.5} Sc^{0.33} \quad (15)$$

In devolatilization, the particle temperature change occurs which is evaluated from energy balance based on radiative, latent and convective heat transfer. After

devolatilization, the char surface reaction with oxygen, carbon dioxide, and water are started, and heat balance for surface reaction is evaluated from equation (17) [49].

$$m_p C_p \frac{dT_p}{dt} = hA_p\left(T - T_p\right) + \frac{dm_p}{dt} L + A_p \varepsilon_p \sigma\left(\theta_R^4 - T_p^4\right) \quad (16)$$

$$m_p C_p \frac{dT_p}{dt} = hA_p\left(T - T_p\right) + f_h \left(\frac{dm_p}{dt}\right) \Delta H + A_p \varepsilon_p \sigma\left(\theta_R^4 - T_p^4\right) \quad (17)$$

3.7.4 Chemical Reaction

For the conservation of species, the equation (18) is applied. The species net production rate R_i, mass rate creation S_i, diffusion flux J_i which is because of concentration temperature gradient. The Arrhenius reaction sum is applied for N_R reaction, and the parameters which are involved are molecular weight $M_{w,i}$, Arrhenius molar rate production per consumption of species in all reaction $\widehat{R_{\iota,r}}$.

$$\nabla.(\rho\vec{v}Y_i) = -\nabla.\vec{J_\iota} + R_i + S_i \quad (18)$$

$$R_i = M_{w,i} \sum_{r=1}^{N_R} \widehat{R_{\iota,r}} \quad (19)$$

3.7.5 Arrhenius rate

The Arrhenius rate is applied for computation of finite-rate/eddy-dissipation model. For the heterogeneous reactions, only finite-rates are used. The reactant and product stoichiometric coefficient are $\nu\,i',r$,$\nu\,i'',r$, rate exponent are , $\eta' j,r$,$\eta' j',r$ respectively ,activation energy E_r, pre-exponential factor A_r, temperature exponent is n and K_k is equilibrium constant, all these parameters are involved in equation (20,21,22)

$$\widehat{R_{\iota,r}} = \left(v_{i,r}^{n} - v_{i,r}'\right)\left(k_{f,r} \prod_{j=1}^{N} [C_j]^{\eta_{j,r}'} - k_{b,r} \prod_{j=1}^{N} [C_j]^{\eta_{j,r}'}\right) \quad (20)$$

$$k_{f,r} = A_r T^n exp(-E_r/RT) \quad (21)$$

$$k_{b,r} = \frac{k_{f,r}}{K_k} \quad (22)$$

3.7.6 Eddy-dissipation rate

For the eddy-dissipation rate, the following equations are applied, the mass fraction is Y_R and Y_P. Magnussen constant, molecular weight, and subscripts for reactant and product are A and B, M and R, P respectively.

$$R_{i,r} = min\left(R_{i,r}^{(R)}, R_{i,r}^{(p)}\right) \quad (23)$$

$$R_{i,r}^{(R)} = v_{i,r}' M_i A \rho \frac{\varepsilon}{k}\left(\frac{Y_R}{v_{R,r}' M_R}\right) \quad (24)$$

$$R_{i,r}^{(P)} = v_{i,r}'' M_i AB \frac{\varepsilon}{k} \left(\frac{\sum PY_P}{\sum_j^N v_{j,r}'' M_j} \right) \quad (25)$$

3.7.7 Radiation model

For the radiative heat transfer equation, the discrete ordinate (DO) radiation model is applied as follow.

$$\frac{dI_{rad}(\vec{r},\vec{s})}{ds} = (a + a_p + \sigma_p) I_{rad}(\vec{r},\vec{s}) + E_p + a\phi^2 \frac{\sigma T^4}{\pi} + \frac{\sigma_s}{4\pi} \int_0^{4\pi} I_{rad}(\vec{r},\vec{s}) \Phi(\vec{s},\vec{s}) d\Omega \quad (26)$$

3.8 Reaction Kinetics

During the gasification, some of the major reactions are devolatilization of volatile matter, char combustion, carbon dioxide gasification, hydrogen gasification, steam gasification, methane oxidation, steam methane reforming, carbon monoxide oxidation, forward and reserve water gas shift reactions, hydrogen oxidation, and tar oxidation are involved. The Arrhenius constant and activation energy along with reactions are given in table (10)

3.8.1 Devolatilization

Fuel feed and oxidizing agent when entering into gasifier it starts mix quickly. Due to the mixing of the moisture present in feed fuel start vaporization rapidly. Devolatilization is the process of leaving of volatile components from solid fuels. The volatile matter mostly consists of hydrogen, carbon monoxide, methane, tar which further react with oxygen and provide the energy for consequent reactions. The char is the solid residue which left after the devolatilization, and the char is consist of carbon and ash. The devolatilization is depended on the gasifier type, operating conditions, the particle size of solid fuel and volatile fraction within the solid fuel.

3.8.2 Coal Gasification Reactions

In almost all types of gasifiers, with different symmetry and principle, following major reactions occur simultaneously [50]. The graphical representation is shown in figure (26). Following significant conclusions are drawn from the figure (26):

i. The curve between $\log_{10}K_p$ and 1/T is almost linear for all the reactions.
ii. The amount of heat necessary for the reaction to proceed (exothermic reaction) is equal to the slope of the curve $\log_{10}K_p$ and 1/T for individual reaction curve.

iii. At low temperature, hydrogasification is preferred thermodynamically for which criteria is $\log_{10}K_p>0$. On the contrary to this carbon dioxide and steam gasification reactions takes place at high temperature.

iv. For WGS reaction, equilibrium constant shows significant variation with temperature change as compared to all other chemical reactions that show little or negligible variation. Equilibrium of WGS reaction can be easily shifted by changing operating parameters as compared with all other reactions in the process[7].

3.8.3 Steam Gasification

The heat input is essential for steam gasification reaction to proceed due to its endothermic nature.to enhance the rate of reaction in limited time steam is supplied in excess [10].The carbon and gaseous reactants mechanistic chemistry is being discussed here precisely, but not for reactions that occur between gaseous reactants and solid carbon. Carbon has the maximum percentage value in coal as it is clear from the proximate analysis of lignite coal. But, the reactivity of carbon is different from other elements and compounds present in coal. In normal practice, pure carbon is less reactive as compared to coal because there is a number of various reactive compounds present in the coal which alters it overall reactivity and they also play a role as a catalyst in many chemical reactions, altering the rate of reaction [50]. Mineral matter present also increases the reactivity of coal depending on the nature of minerals present. Anthracite has the highest percentage of carbon in proximate analysis and is best in rank among all types of coal but offers the least reactivity and is most unlikely and difficult to gasify or liquefy because it requires lots of heat and elevated temperatures to gasify this solid fuel. The carbon deposition reaction occurs at a good rate when steam supplied in the gasifier is low [5].

3.8.4 Carbon Dioxide Gasification

The reaction between carbon and carbon dioxide produced in combustion reaction is known as a Boudouard reaction. This reaction is of endothermic nature and requires heat to proceed similarly to the steam gasification reaction [2].

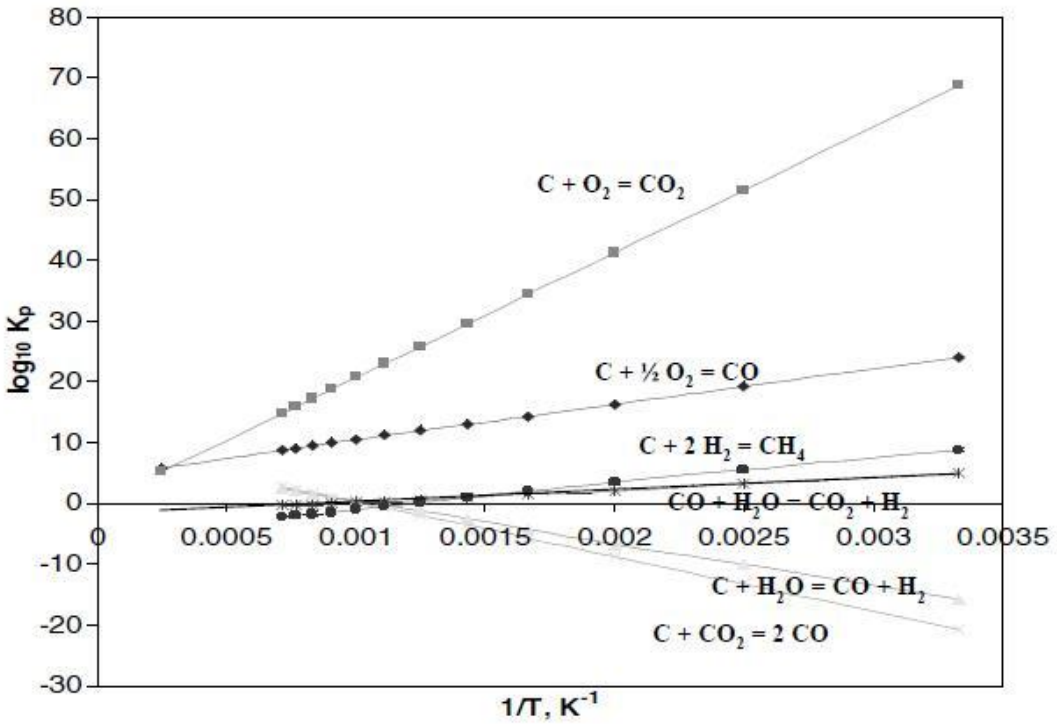

Figure 26 Plot Between 1/ T and log10Kp

For reaction to occur separately, it requires very high temperature and pressure (for reaction rate to be satisfactory). When reactant concentrations are higher than normal high pressure is required to get maximum conversion[2, 7].The Boudouard reaction is difficult to be carried out separately as it is not cost-effective; highly energy intensive, slow reaction rate problem and minimum conversion are the major problems that practically arise. Methane can also be produced by addition of hydrogen gas to the lignite coal at very high operating pressures. The reaction is commonly termed as hydro gasification [51].

The reaction mentioned above generates heat in that it is preferred at low operating temperature because of the exothermic nature. The temperature preferred for the reaction below 670°C, which is opposite to the steam and carbon dioxide gasification reactions [12]. At low, to moderate temperatures, the other problem that arises is slow reaction rate. Thus, for reaction rates being high and better kinetics of process temperature is kept on the higher side. For syngas production, high pressure shifts the equilibrium in syngas formation. The overall cost and economics of process increase with the use of a catalyst, making difficult to justify the process on economic grounds because the exhausted catalyst recovery posse a serious problem and its recycling also

require energy and cost for the removal of unreacted char and ash and regeneration [50].Consequently, the above-mentioned complications are the main reasons due to which catalytic gasification is not practiced widely on a commercial scale [8]

3.8.5 Partial Oxidation

Coal combustion reaction with oxygen, which can be provided as pure or a fraction of air results in carbon monoxide and carbon dioxide.

If the amount of air or oxygen supplied is just sufficient or stoichiometrically required, then vapor- phase oxidation and ignition of volatile matter are the phenomena by which combustion proceeds sequentially and eventually leading towards the ignition of residual char. To continue combustion reaction for a long-time result in the inadequate use of carbonaceous solid, that's why it is not desirable. Although the expressions for combustion and oxidation reactions are a simple equation, the partial oxidation mechanism is complex and which depends on how quickly and efficiently combustion reaction proceeds [11].Due to the presence of both heterogeneous and homogeneous reactions the pathway of the main reaction is further complicated to understand. The early argument that arises in carbon oxidation reaction is whether in the heterogeneous reaction of oxygen and carbon the main product is carbon dioxide, or the other suppressed product is carbon monoxide in gas phase oxidation reaction [7].

3.8.6 Water Gas Shift (WGS) Reaction

WGS reaction is not the prime centered reaction in gasification reactions, yet its importance in chemical reaction systems and synthesis gas is very much significant. The equilibrium for WGS reaction is least sensitive among all other reactions when temperature variation is considered [2, 7] . It can be concluded with other words that its equilibrium constant has almost no effect of temperature change. Thus, equilibrium for WGS reaction does not shift for a long range of temperature variation in operation. WGS reaction when proceeds in the forward direction is slight of exothermic nature [2].

Scientists and chemist still have believed that reaction takes place at the coal particle surface and is of heterogeneous type and is catalyzed by solid carbon surface. However, on the other hand, all the chemical species participating in the reaction are in gaseous state. It is difficult to understand and develop a generalized approach

regarding WGS reaction as it is being catalyzed on heterogeneous surfaces. Also, the reaction is homogeneous and heterogeneous. For commercial scale reactor, the rate kinetics information available in the literature is not of much use and worth. Methanol production from syngas can be achieved by keeping the hydrogen and carbon mono oxide ratio 2:1 and operating the gasifier at low pressure especially in vapor phase [8]. Balanced gas is a term used for consistent syngas produced from above methodology on the other hand syngas composition that differs from basic principle reactions is known as unbalanced syngas [51].If the high yield of hydrogen is required in syngas, then hydrogen to carbon monoxide ratio should be further increased by mainly GS reaction and convert maximum, produced CO into carbon monoxide. If the hydrogen produced by syngas mixture is to be used in fuel cell applications, carbon monoxide and carbon dioxide should be removed to the minimum level by adsorption process or either employing acid gas removal unit.

3.8.7 Reaction Kinetics Char Reactions

Reactions (R3-R5) are the solid-gas reactions involving solid carbon as a reactant in char with the gasifying medium. Some of these reactions are volumetric reactions, while others are surface reactions. In the volumetric reactions, gas can quickly diffuse into the particles and reaction takes place throughout the interior of the particle as diffusion rate is much more as compared to the reaction rate. In the surface reaction, gas does not penetrate into the pores and spaces inside the particle but rather is confined at the surface of the shrinking core of unreacted solid. Generally, the volumetric reaction occurs when a chemical reaction is slow compared with diffusion. The surface reaction occurs when a chemical reaction is very fast and diffusion is the rate-limiting step. Among these four reactions, the rate of reaction (R2) is fast compared to the diffusion rate of reactants, so the reaction (R2) occurs spontaneously on the surface of solid particles of char. The rates of the other reactions are rather slow compared with the reaction (R2) because of the low operating temperature in the coal gasifier, typically lower than the ash fusion temperature.

Table 10 Reactions

S.NO	Reactions	A	Ea $\times e^{+08}$ (J/Kmol)	References
R1	$vol \rightarrow aCo + bH_2 + cCH_4 + dH_2O + eH_2S + fO_2 + gN_2 + hTar$	2.119e^{+11}	2.027	[52]
R2	Char Combustion $C < S > +0.5O_2 \longrightarrow CO$	300	1.3	[38]
R3	CO_2 Gasification $C < S > +CO_2 \longrightarrow 2CO$	2244	2.2	[38]
R4	H_2 Gasification $C < S > +H_2 \longrightarrow CH_4$	1.62	1.5	[38]
R5	H_2O Gasification $C < S > +H_2O \longrightarrow CO + H_2$	42.5	1.42	[38]
R6	Methane Oxidation $CH_4 + 1.5O_2 \longrightarrow CO + H_2O$	5.012e^{+11}	2	[52]
R7	Steam methane reforming $CH_4 + H_2O \longrightarrow CO + 3H_2$	5.92 e^{+08}	2.09	[53]
R8	CO oxidation $CO + 0.5O_2 \longrightarrow CO_2$	2.239 e^{+12}	1.7	[52]
R9	Forward water-gas shift reaction $CO + H_2O \longrightarrow CO_2 + H_2$	2.35 e^{+10}	2.88	[52]
R10	Reverse water-gas shift reaction $CO_2 + H_2 \longrightarrow CO + H_2O$	1.785e^{+12}	3.26	[52]
R11	Hydrogen Oxidation $H_2 + 0.5O_2 \longrightarrow H_2O$	9.87e^{+8}	0.31	[52]
R12	Reverse Hydrogen Oxidation $H_2O \longrightarrow 0.5O_2 + H_2$	2.06 e^{+11}	2.72	[52]
R13	Tar Oxidation $Tar + O_2 \longrightarrow CO$	1e^{+15}	1	[54]

Chapter 4

Results and Discussion

4.1 Single stage Gasifier

Fig (27-31) shows the contours of mass fractions of carbon monoxide, hydrogen, water, carbon dioxide, oxygen. From the results, it is analyzed that in single stage gasifiers where the mass fraction of carbon dioxide is high carbon monoxide is low but along the length due to char reactions of carbon monoxide and water the mass fraction of carbon dioxide is increased and carbon dioxide is decreased. The oxygen is the oxidizing agent, so in the injection points the mass fraction of oxygen is high, but after that due to combustion reactions the oxygen is utilized in to formation of carbon dioxide and water but after that along the length the mass fraction of oxygen is decreased so in the presence of limited oxygen the endothermic reactions occur, and hydrogen production is increases.

The figure (32-33) show the velocity and temperature profile. At the injection point of air, the velocity is more, but along the length, it starts decreases when the reactions occur. From the temperature profile, it is observed that almost at the center of the reactor the exothermic reactions occur so in that region the temperature is high, but after that along the length, the temperature start decreases due to endothermic reactions. Figure (34) show the residence time of particles and point out that the particles residence time is almost 0.17 seconds in the reactor during which all the reactions take place.

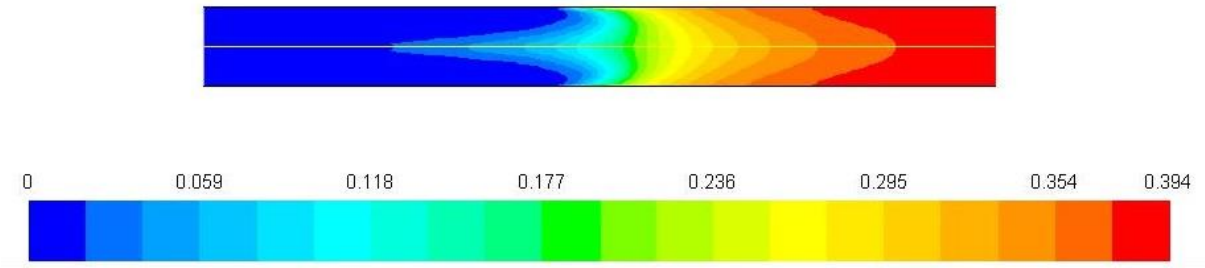

Figure 27 Mass fraction of carbon monoxide

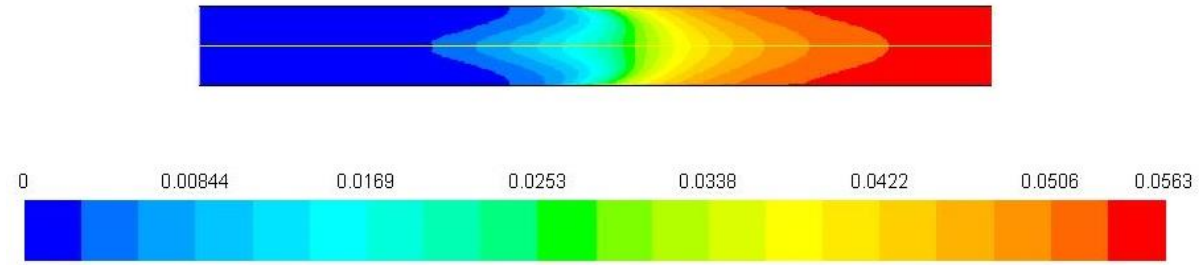

Figure 28 Mass fraction of hydrogen

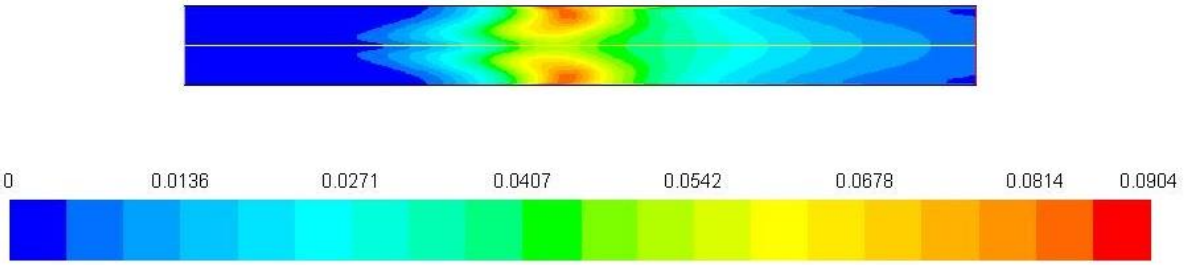

Figure 29 Mass fraction of carbon dioxide

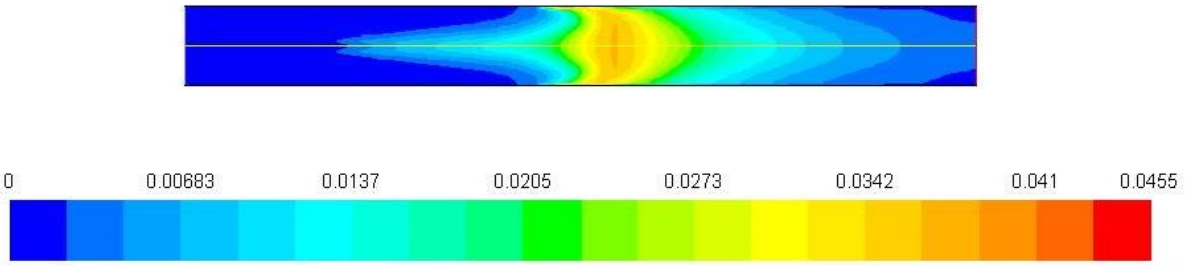

Figure 30 Mass fraction of water

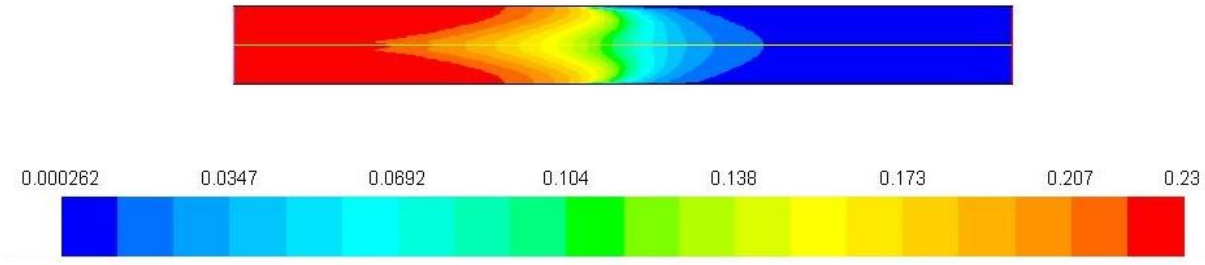

Figure 31 Mass fraction of oxygen

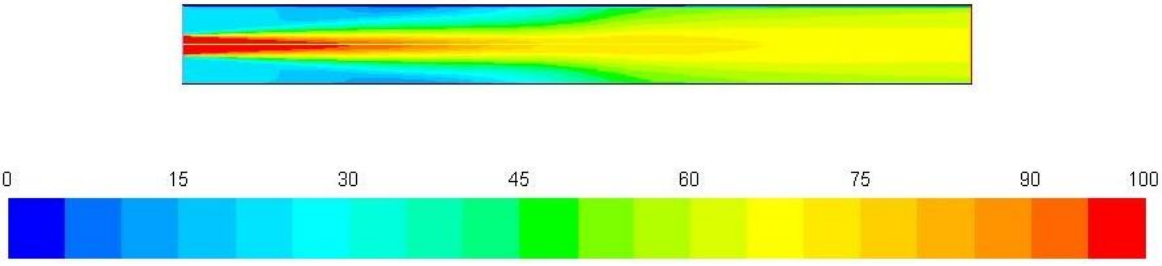

Figure 32 Velocity profile

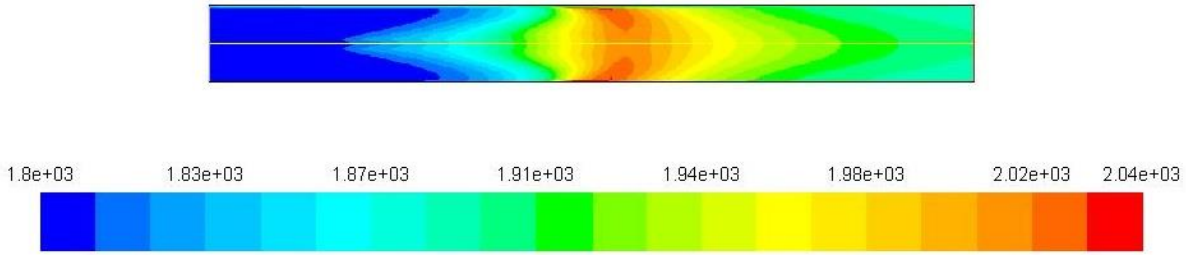

Figure 33 Temperature profile

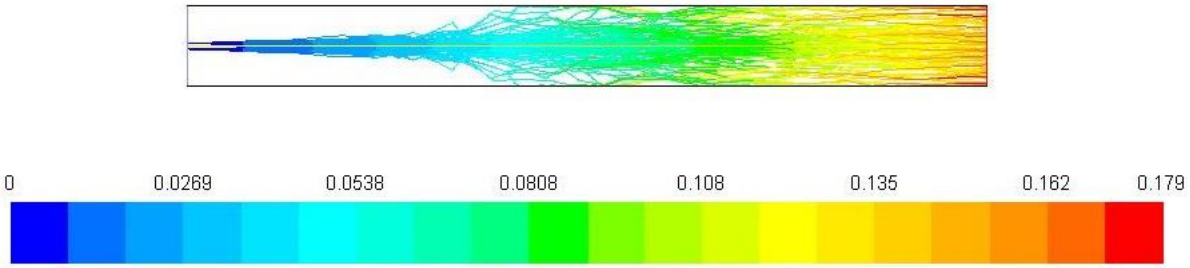

Figure 34 Residence time

4.2 E-gas entrained flow gasifier

Contours of the magnitude of velocity are shown in figure (35). From the contours, it is examined that with respect to the second stage of the gasifier the velocity profile remains symmetric. Figure (36) shows the contours of temperature, from the contours it is observed that temperature is decreased in the second stage of gasifier as compared to the first stage. Figure (37) show the pressure profile of reactor that operating pressure remains constant throughout the gasifier. This reduction in temperature is because of the endothermic reaction of char gasification. The contours of oxygen mole fraction show that jet penetration is done at both ends of 1st stage gasifier as shown in figure (38). The boundary conditions, stoic-metric ratio and buoyancy effect, turbulence and fluid dynamics may affect the penetration length. The contours of water mole fraction are shown in figure (39). At the oxygen injection point the mole fraction of water is high, and up to the second stage, slurry injection makes the reduction in mole fraction because of water gas shift reaction and water reaction with char in char gasification. Figure (40) show the mole fraction contours of carbon dioxide. From the contours, it is examined that at high temperature the mole fraction of carbon dioxide is high the mole fraction of carbon dioxide is decreased along the height of gasifier because of carbon dioxide reaction with char. Figure (41) show the contours of mole fraction of carbon monoxide. The mole fraction of CO is less in the 1st stage, but it increases in the 2nd stage of gasifier because of char reaction with carbon dioxide and water. Figure (42) show the contours of hydrogen. For contours, it is found that the

hydrogen mole fraction is high at high-temperature region mean in 1st stage and it decreases along the height. This is due to water gas shift reaction and methane reaction. The reduction in hydrogen mole fraction in 2nd stage may be due to slurry injection and forward water shift reaction. The methane mole fraction in the 1st stage in less as compared to the 2nd stage because of the 1st stage the temperature, high and at high temperature the methane oxidation and steam reforming reaction occur but in 2nd stage, these reactions do not fully occur and it leads to methane mole fraction is high at the exit shown in figure (43).

Figure (44,45,46) show the mole fraction of hydrogen sulfide, tar, and nitrogen. From the contours of hydrogen sulfide, it is observed that due to devolatilization reactions there is a limited production of hydrogen sulfide occurs due to the presence of sulfur in the feedstock. From contours of tar, it is analyzed that in the 1st stage due to high temperature the tar formation is more, but the temperature is a drop in the 2nd stage, so tar production decreases. As there is no reaction of nitrogen involved in the simulation process, so there is limited nitrogen which is present in feedstock leave the gasifier without any notable change and act as a carrier for other gases.

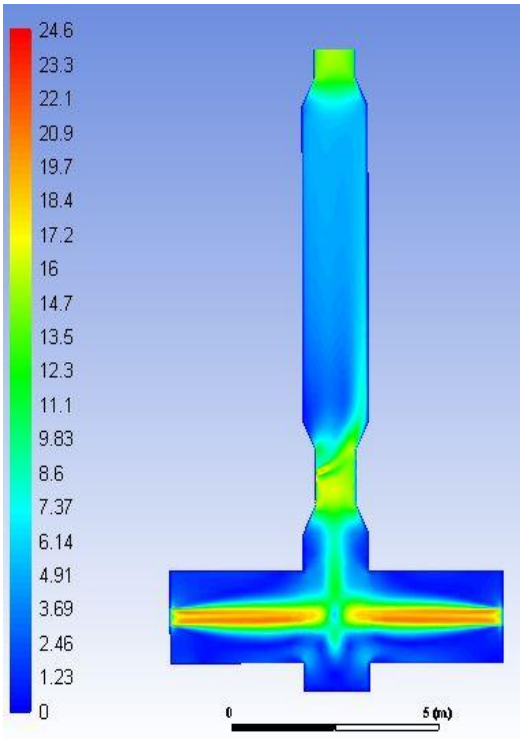

Figure 35 Velocity profile

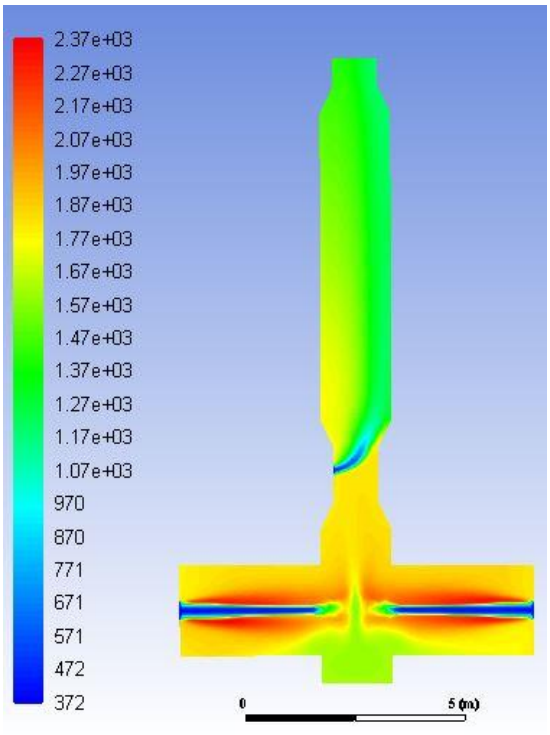

Figure 36 Temperature Profile

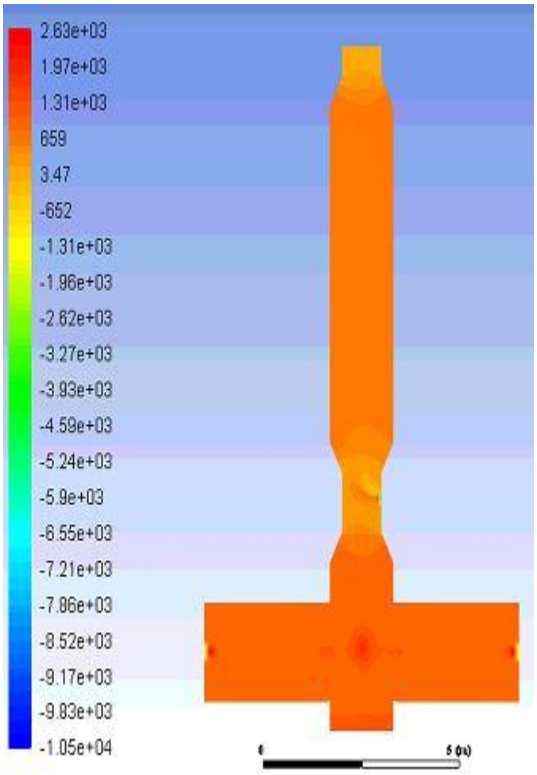

Figure 37 Pressure

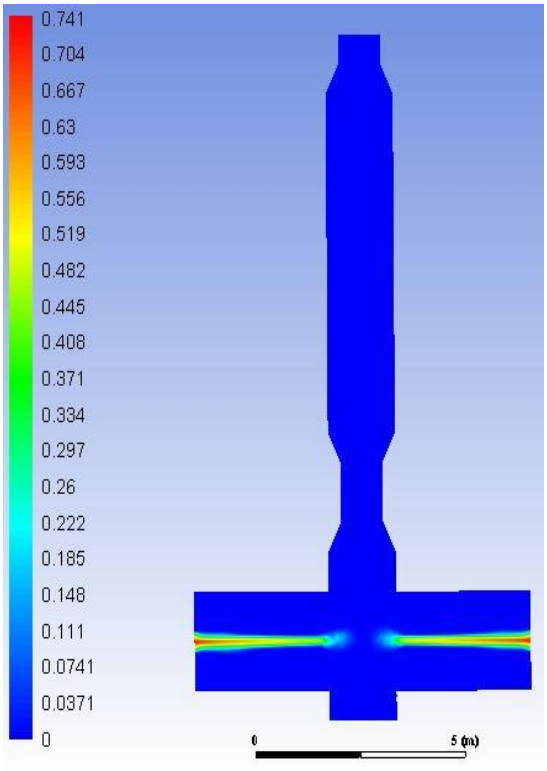

Figure 38 Oxygen mole fraction

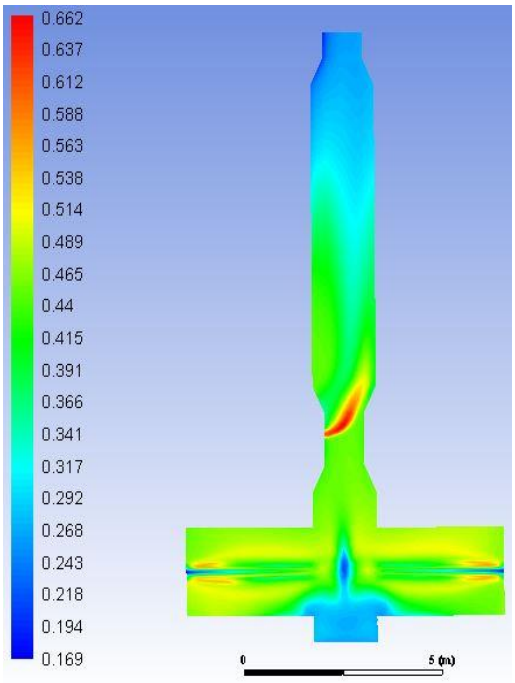

Figure 39 Water mole fraction

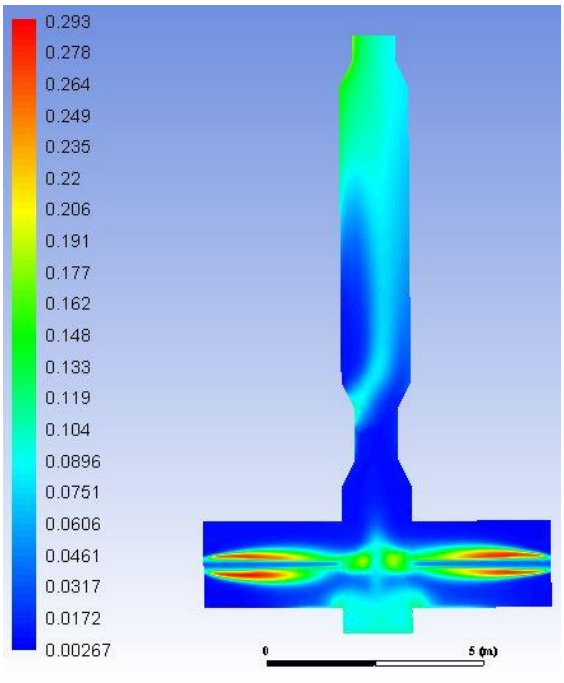

Figure 40 Carbon dioxide mole fraction

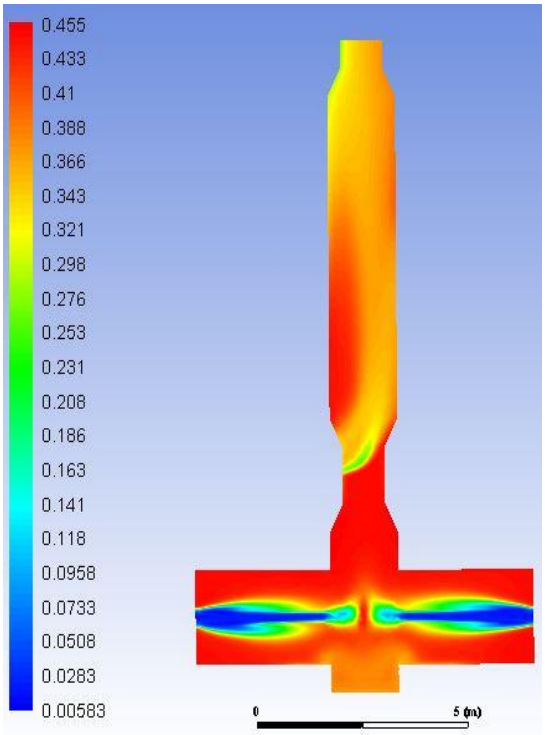

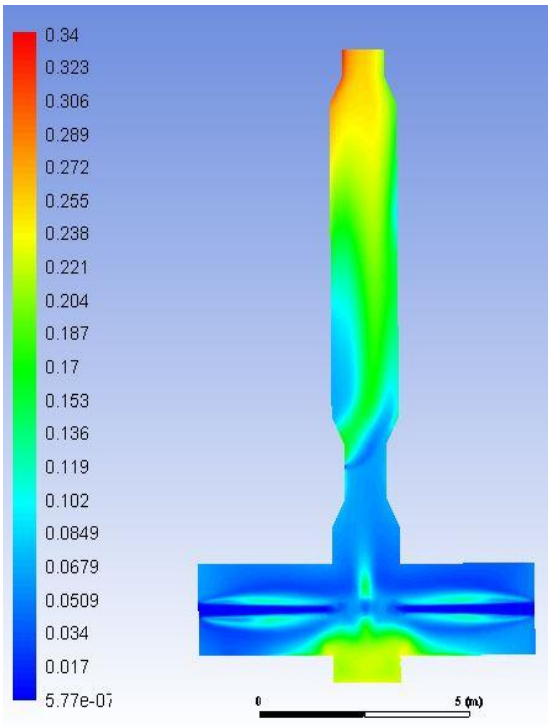

Figure 41 Carbon monoxide mole fraction

Figure 42 Hydrogen mole fraction

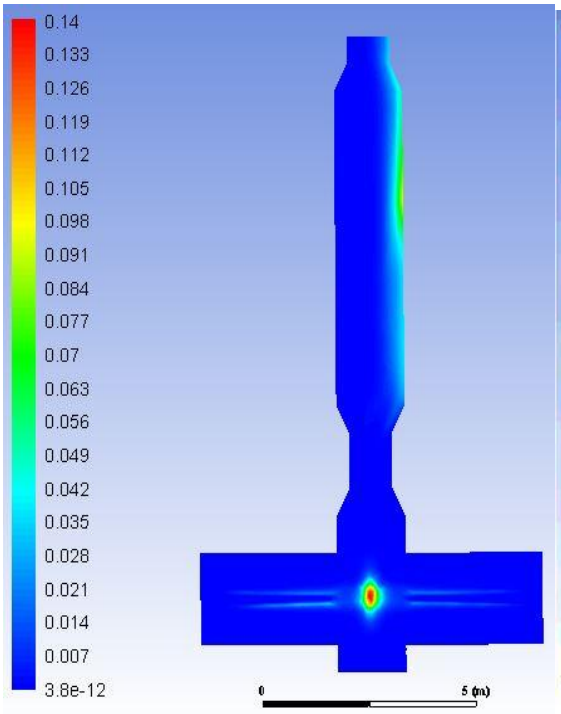

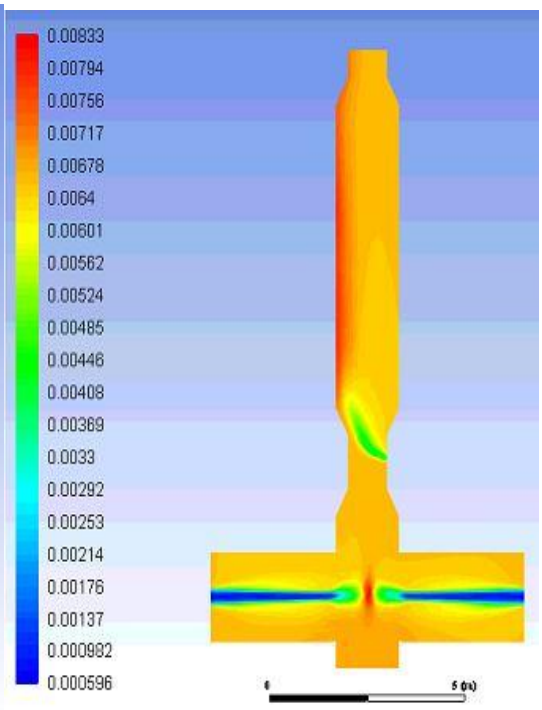

Figure 43 Methane mole fraction

Figure 44 Hydrogen Sulfide mole fraction

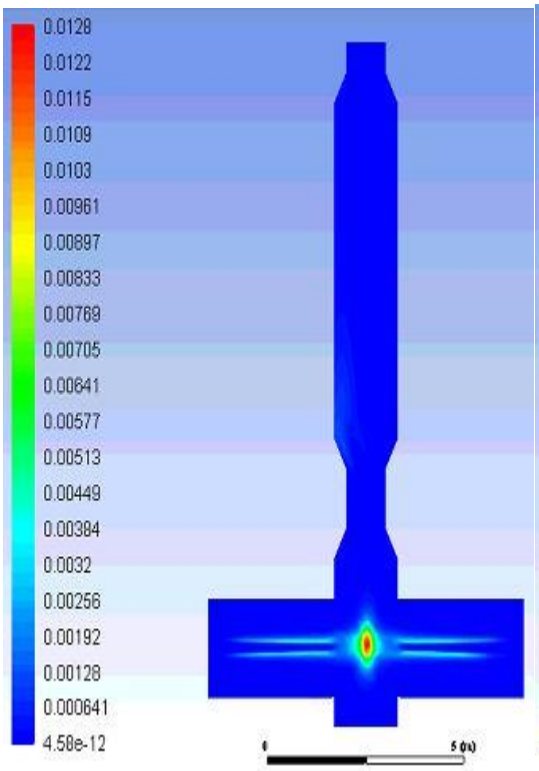

Figure 45 Tar mole fraction

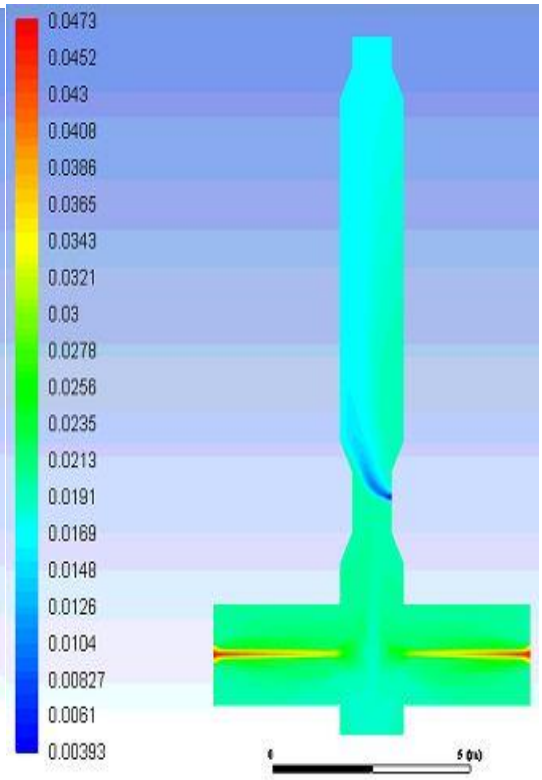

Figure 46 Nitrogen mole fraction

4.2.1 Validation of E-gas gasifier model results

Table 11 Syngas Composition

Percentage dry volume fraction			
	Model Values	Wabash River Plant	% Change
CO	45.40	45.30	0.22
CO2	13.72	15.80	13.16
H2	37.61	34.4	9.33

4.3 Air blown Entrained flow gasifier

The mass fraction of carbon monoxide is lower in combustion zone because of excess of oxygen and combustion reactions but when diffuser chamber comes to the amount of carbon monoxide increase because here low oxygen as compared to combustion zone but in redactor or 2nd stage the mass fraction of carbon monoxide increase due to reduction reactions in the presence of limited oxygen as shown in Figure (47).The mass fraction of hydrogen is increased in the combustion chamber due to a high temperature, but it is less in the diffuser zone after that because of limited oxygen, and

a reduction reaction occurs due to this the hydrogen increases in reduction zone as shown in Figure (48).

Figure (49) show the mass fraction of carbon dioxide contours. From the contours, it is observed that as in combustion zone the temperature is high and oxygen concentration is high due to which the mass fraction of carbon dioxide is high in this zone. But in diffuser and redactor zone the oxygen is limited, and because of carbon dioxide and char reactions, the mass fraction of carbon dioxide decreases.

The contour of mass fraction of water is shown in figure (50). From the contours, it is analyzed that in combustion zone due to combustion process the mass fraction is more as compare to redactor zone because in redactor zone due to water gas shift reaction and water reaction with char in the gasification process.

Figure (51) show the mass fraction of methane. In the combustion zone, the methane mass fraction is less as compare to redactor zone. This is due to methane oxidation, steam reforming reaction at high temperature in combustion zone but these reactions slow done in redactor zone, so methane mass fraction is high at the exit. The contour of oxygen is shown in figure (52). The contours reveal that mass fraction of oxygen at the injection point is high, but after that due to reactions in combustion, diffuser and redactor zone, the mass fraction of oxygen is decreased.

Figure (53) show the mass fraction of nitrogen. As in this simulation, the no nitrogen reaction is involved. So, in this process, it acts as a carrier of gases to move in upward direction. So, in the whole gasifier, the mass fraction of nitrogen remains unchanged.

Figure (54) show the mass fraction of tar formation in the gasifier. As in the combustion zone, the temperature is high, so the tar formation is less, but after that, the temperature is dropping so there is limited tar production occur in the gasifier.

Figure (55) show the contours of mass fraction of hydrogen sulfide. During the devolatilization reaction of volatile matter, there is a limited production of hydrogen sulfide due to the presence of volatile sulfur matter. The temperature profile in figure (56) shows that in combustion zone the temperature is high but along the height the gasifier height the temperature is decreased due to endothermic char reactions. The operating pressure profile is shown in figure (57). As in the simulation, the pressure is

adjusted at optimum conditions of 2.7MPa. The contour shows that throughout pressure no change in operating pressure.

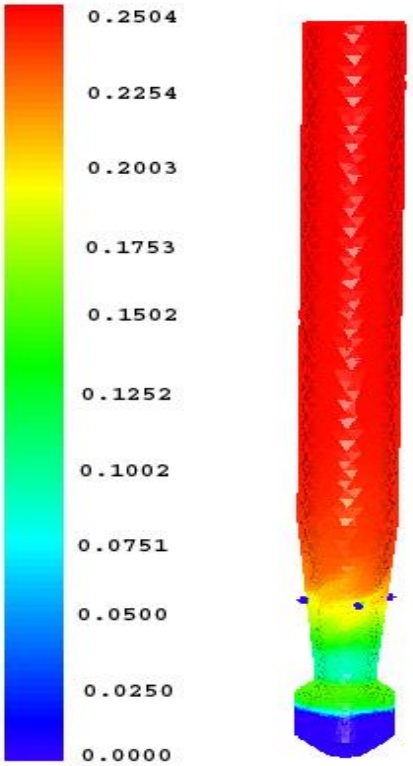

Figure 47 Mass fraction of CO

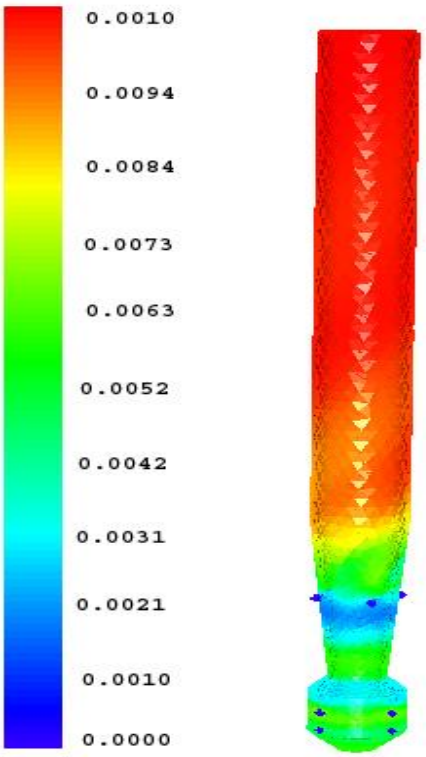

Figure 48 Mass fraction of H_2

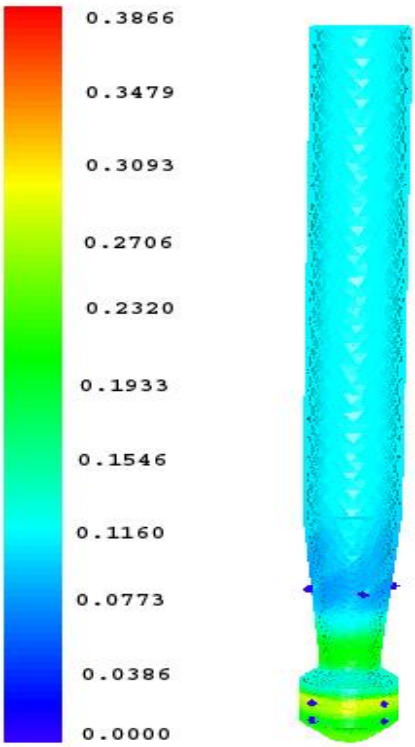

Figure 49 Mass fraction of CO_2

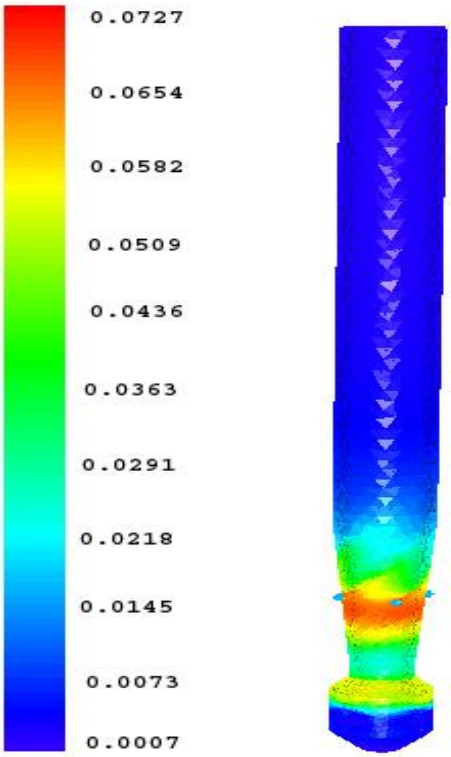

Figure 50 Mass fraction of H_2O

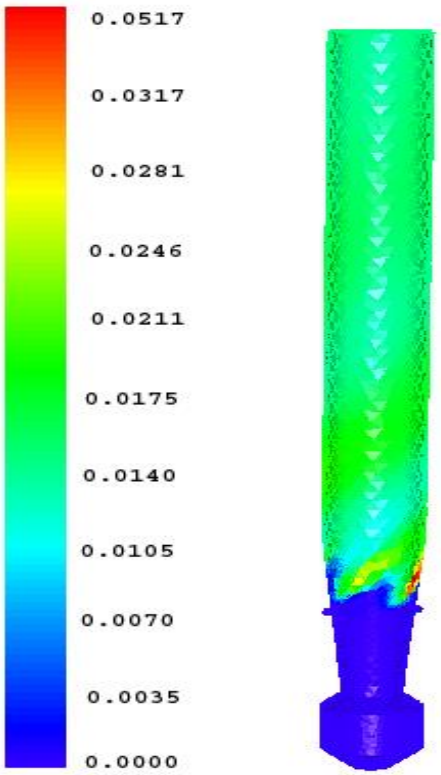

Figure 51 Mass fraction of CH_4

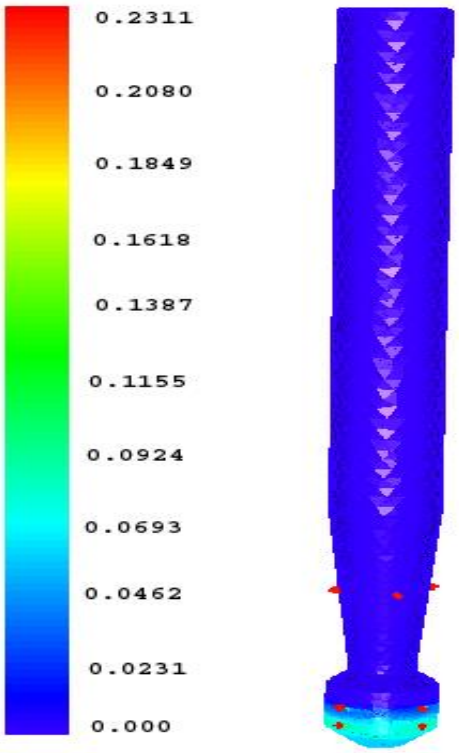

Figure 52 Mass fraction of O_2

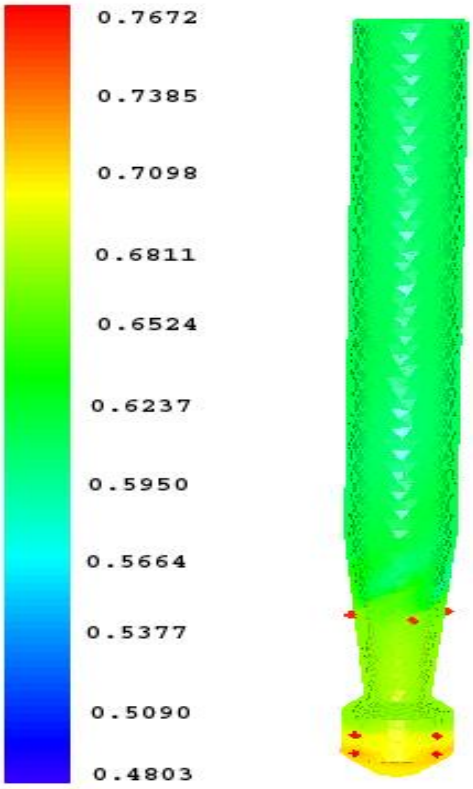

Figure 53 Mass fraction of N_2

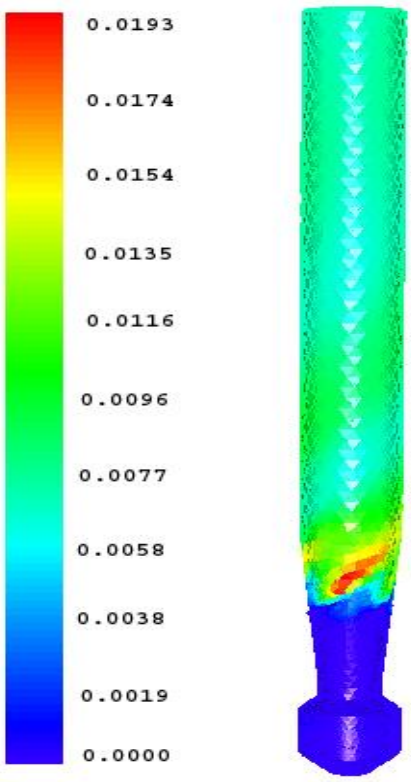

Figure 54 Mass fraction of tar

Figure 55 Mass fraction of H_2S

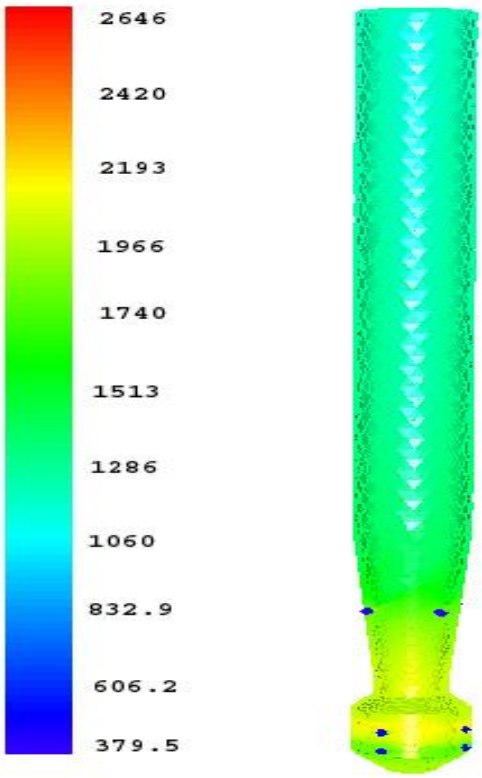

Figure 56 Temperature Profile

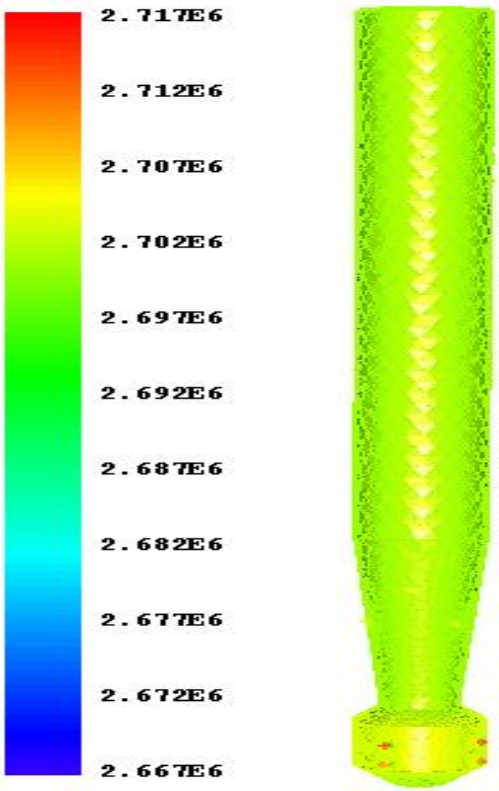

Figure 57 Pressure Profile

4.3.1 Validation of air blown entrained flow gasifier model results

The graph of carbon monoxide, carbon dioxide, hydrogen mole fractions comparison with the literature data is shown in figure (58,59,60). From the graph of CO mole fraction, it is observed that along the gasifier the carbon monoxide mole fraction is increased due to gasification reactions in redactor zone of gasifier. Carbon dioxide is decreased along the gasifier height because at the lower stage or in the combustion zone of gasifier the combustion reactions occur but along the gasifier height and in redactor zone the carbon dioxide is converted into other products that is why it decreases along the height. The hydrogen mole fraction in the lower part of the gasifier is low as compared to upper zone this is because high temperature at lower region but at upper region the temperature decreases and limited oxygen so reduction reactions occur and produce hydrogen. The graph of temperature is shown in figure (61). It reveals that due to exothermic reaction at lower zone mean in combustion zone the temperature becomes high but after that endothermic reactions start along with exothermic reactions, so temperature becomes relatively low. Figure (62) show that the model results almost validated the literature results.

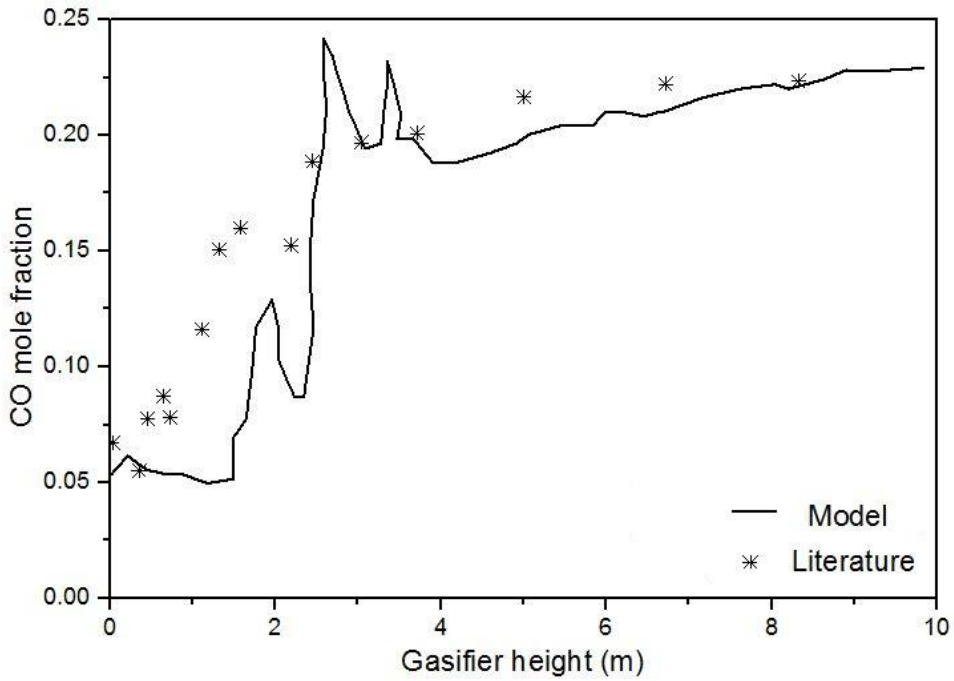

Figure 58 Carbon monoxide mole fraction

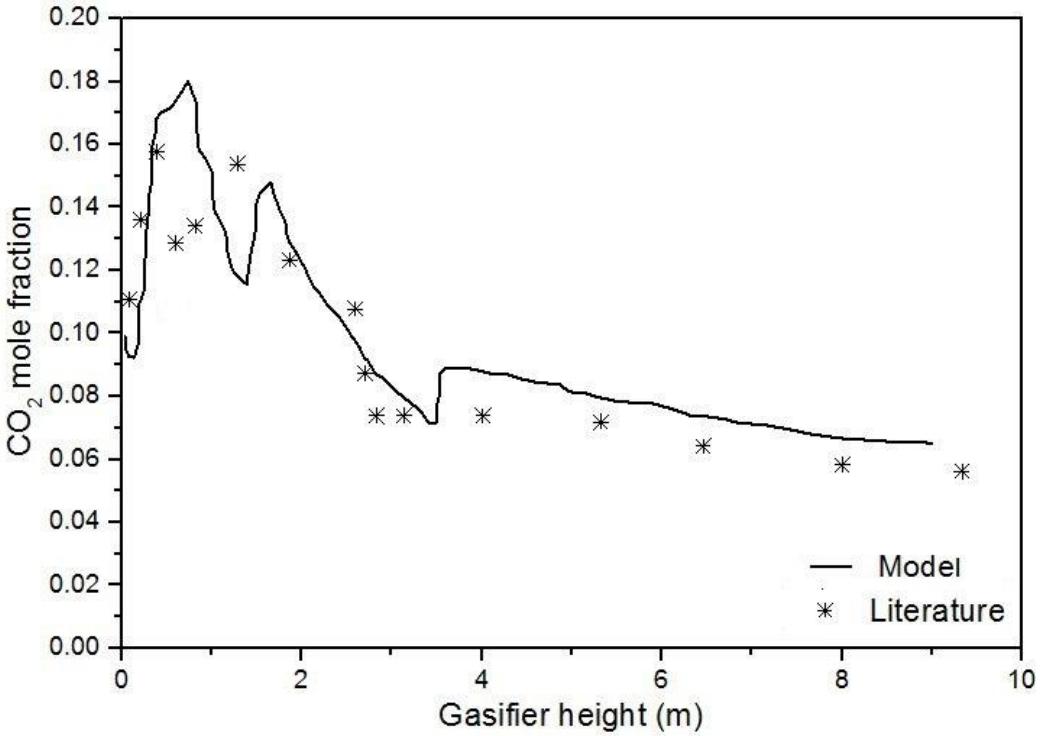

Figure 59 Carbon dioxide mole fraction

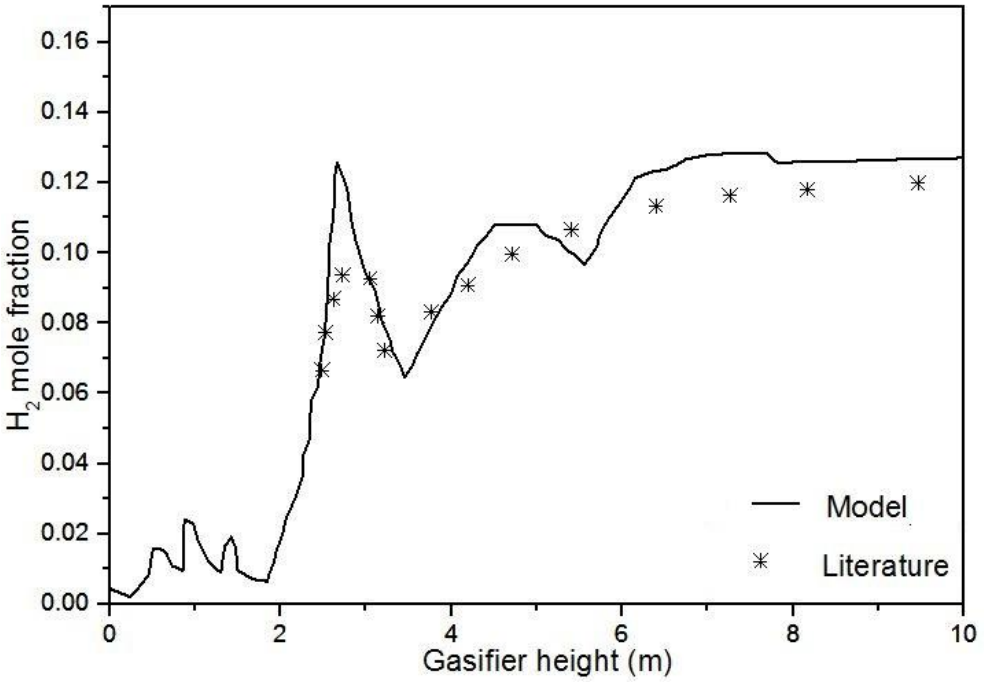

Figure 60 Hydrogen mole fraction

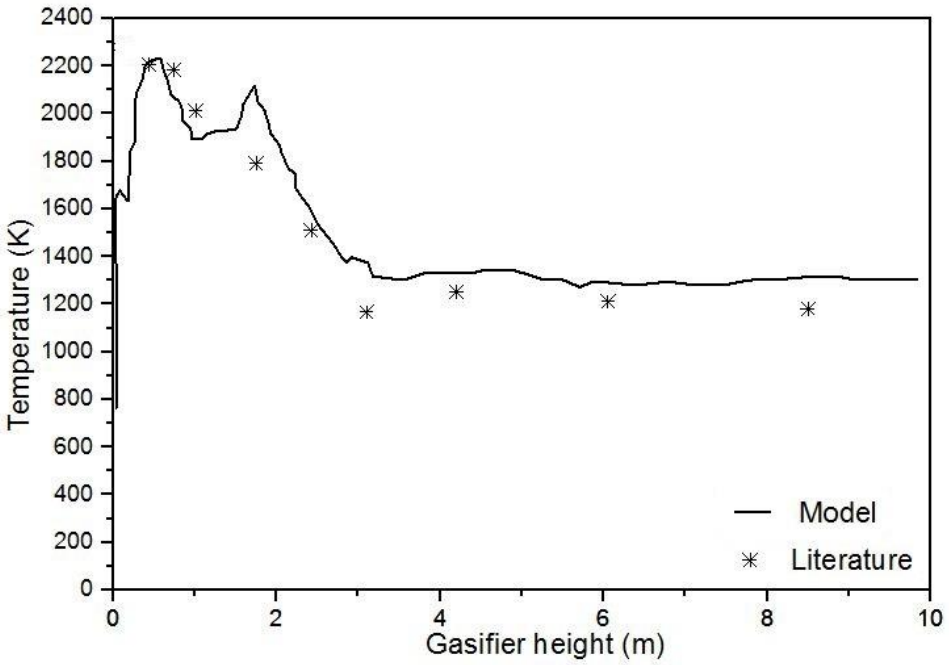

Figure 61 Temperature

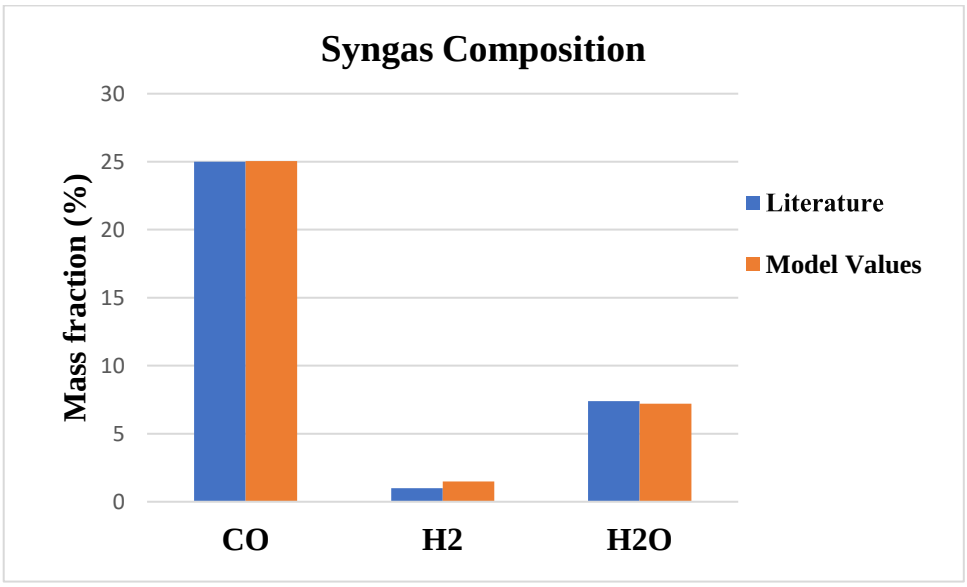

Figure 62 Syngas Composition

Conclusions

In the present research, the CFD analysis is done for the entrained flow gasifier by using bituminous coal as feedstock. The sub-models related to coal devolatilization, combustion and gasification are applied for better syngas composition in the product. The volatile matter includes not only major combustion and gasification species but also include minor species such as H_2S and tar. Almost thirteen reactions are incorporated in this model from which four are surface reactions, and others are gas phase reactions. The approach used to ensure an optimum convergence for energy and mass conservation for discrete species in CFD model. The predicted temperature velocity and syngas composition containing mole fraction of carbon monoxide, hydrogen, carbon dioxide, methane provide a reasonable trend for the gasifier. The accuracy of predicated syngas composition is almost within range of experimental results. From the analysis is examined that at the exit the syngas composition is not in chemical equilibrium due to heterogeneous and homogeneous gas phase reactions kinetics.

Future Recommendations

- ✓ CFD of other commercial entrained flow gasifiers.
- ✓ Exergy analysis of entrained flow gasifier based on computational fluid dynamics
- ✓ Modeling and simulation of entrained flow gasifier based on ASPEN model to evaluate the syngas composition, cost analysis, exergy analysis of gasifier.
- ✓ Computational fluid dynamics of coal and other fuels such as biomass as combine feedstock for the entrained flow gasifier.

References

[1] E.A. Council, Integrated Energy Plan 2009-2022: Report of the Energy Expert Group, Ministry of Finance, Government of Pakistan, Islamabad (2009).
[2] S. Lee, J.G. Speight, S.K. Loyalka, Handbook of alternative fuel technologies, crc Press2014.
[3] A. Araújo, M. Bezzeghoud, M. Collares-Pereira, A. Reis, R. Rosa, A. Silva, The IV International Conference on Oil and Gas Depletion, (2005).
[4] J.L. Johnson, Kinetics of coal gasification: a compilation of research, (1979).
[5] X. Lu, T. Wang, Water–gas shift modeling in coal gasification in an entrained-flow gasifier–Part 2: Gasification application, Fuel 108 (2013) 620-628.
[6] B. Board, Bp Board Annual Report 2012, (2012).
[7] G.R. Kale, B.D. Kulkarni, R.N. Chavan, Combined gasification of lignite coal: Thermodynamic and application study, Journal of the Taiwan Institute of Chemical Engineers 45(1) (2014) 163-173.
[8] M. Hobbs, P. Radulovic, L. Smoot, Combustion and gasification of coals in fixed-beds, Progress in Energy and Combustion Science 19(6) (1993) 505-586.
[9] C.Y. Wen, T.Z. Chaung, Entrainment Coal Gasification Modeling, Industrial & Engineering Chemistry Process Design and Development 18(4) (1979) 684-695.
[10] M. Kulkarni, R. Ganguli, Moving bed gasification of low rank Alaska coal, Journal of Combustion 2012 (2012).
[11] C. Wen, H. Chen, M. Onozaki, User's manual for computer simulation and design of the moving-bed coal gasifier. Final report, West Virginia Univ., Morgantown (USA). Dept. of Chemical Engineering, 1982.
[12] A. Plus, Aspen plus model for moving bed coal gasifier, Aspen Technology, Inc., Cambridge, MA, 2010.
[13] A. Bridgwater, The technical and economic feasibility of biomass gasification for power generation, Fuel 74(5) (1995) 631-653.
[14] D. Kunii, O. Levenspiel, Fluidization engineering, Elsevier2013.
[15] A. Labbafan, H. Ghassemi, Numerical modeling of an E-Gas entrained flow gasifier to characterize a high-ash coal gasification, Energy Conversion and Management 112 (2016) 337-349.
[16] H.-H. Lee, J.-C. Lee, Y.-J. Joo, M. Oh, C.-H. Lee, Dynamic modeling of Shell entrained flow gasifier in an integrated gasification combined cycle process, Applied Energy 131 (2014) 425-440.
[17] G. Cau, D. Cocco, F. Serra, Energy and cost analysis of small-size integrated coal gasification and syngas storage power plants, Energy Conversion and Management 56 (2012) 121-129.
[18] B. Zhang, Z. Ren, S. Shi, S. Yan, F. Fang, Numerical analysis of gasification and emission characteristics of a two-stage entrained flow gasifier, Chemical Engineering Science 152 (2016) 227-238.
[19] G. Cau, R. Carapellucci, D. Cocco, Thermodynamic and environmental assessment of integrated gasification and methanol synthesis (IGMS) energy systems with CO2 removal, Energy Conversion and Management 38 (1997) S179-S186.
[20] I.N. Unar, L. Wang, A.G. Pathan, R.B. Mahar, R. Li, M.A. Uqaili, Numerical simulations for the coal/oxidant distribution effects between two-stages for multi opposite burners (MOB) gasifier, Energy Conversion and Management 86 (2014) 670-682.
[21] D. Bi, Q. Guan, W. Xuan, J. Zhang, Combined slag flow model for entrained flow gasification, Fuel 150 (2015) 565-572.
[22] L. Zheng, E. Furinsky, Comparison of Shell, Texaco, BGL and KRW gasifiers as part of IGCC plant computer simulations, Energy Conversion and Management 46(11) (2005) 1767-1779.
[23] J. McGee, R. Taplin, The Asia–Pacific partnership on clean development and climate: A complement or competitor to the Kyoto protocol?, Global Change, Peace & Security 18(3) (2006) 173-192.

[24] S. Xu, Y. Ren, B. Wang, Y. Xu, L. Chen, X. Wang, T. Xiao, Development of a novel 2-stage entrained flow coal dry powder gasifier, Applied Energy 113 (2014) 318-323.
[25] C. Ghenai, I. Janajreh, CFD analysis of the effects of co-firing biomass with coal, Energy Conversion and Management 51(8) (2010) 1694-1701.
[26] I. Janajreh, M. Al-Shrah, Numerical and experimental investigation of downdraft gasification of wood chips, Energy Conversion and Management 65 (2013) 783-792.
[27] H. Watanabe, K. Tanno, H. Umetsu, S. Umemoto, Modeling and simulation of coal gasification on an entrained flow coal gasifier with a recycled CO2 injection, Fuel 142 (2015) 250-259.
[28] F. Emun, M. Gadalla, L. Jiménez, Integrated Gasification Combined Cycle (IGCC) process simulation and optimization, Computer Aided Chemical Engineering, Elsevier2008, pp. 1059-1064.
[29] H.C. Frey, N. Akunuri, Probabilistic modeling and evaluation of the performance, emissions, and cost of texaco gasifier-based integrated gasification combined cycle systems using ASPEN, Prepared by North Carolina State University for Carnegie Mellon University and US Department of Energy, Pittsburgh, PA (2001).
[30] E. Chui, A. Majeski, D. Lu, R. Hughes, H. Gao, D. McCalden, E. Anthony, Simulation of entrained flow coal gasification, Energy Procedia 1(1) (2009) 503-509.
[31] G.-S. Liu, H. Rezaei, J. Lucas, D. Harris, T. Wall, Modelling of a pressurised entrained flow coal gasifier: the effect of reaction kinetics and char structure, Fuel 79(14) (2000) 1767-1779.
[32] C. Chen, M. Horio, T. Kojima, Numerical simulation of entrained flow coal gasifiers. Part II: effects of operating conditions on gasifier performance, Chemical Engineering Science 55(18) (2000) 3875-3883.
[33] C. Chen, M. Horio, T. Kojima, Numerical simulation of entrained flow coal gasifiers. Part I: modeling of coal gasification in an entrained flow gasifier, Chemical Engineering Science 55(18) (2000) 3861-3874.
[34] S. Nagpal, T. Sarkar, P. Sen, Simulation of petcoke gasification in slagging moving bed reactors, Fuel processing technology 86(6) (2005) 617-640.
[35] C. Wen, T. Chaung, Entrainment coal gasification modeling, Industrial & Engineering Chemistry Process Design and Development 18(4) (1979) 684-695.
[36] S. Shi, C. Guenther, S. Orsino, Numerical Study of Coal Gasification Using Eulerian-Eulerian Multiphase Model, (42738) (2007) 497-505.
[37] R. Radmanesh, J. Chaouki, C. Guy, Biomass gasification in a bubbling fluidized bed reactor: Experiments and modeling, AIChE Journal 52(12) (2006) 4258-4272.
[38] Y. Wu, P.J. Smith, J. Zhang, J.N. Thornock, G. Yue, Effects of Turbulent Mixing and Controlling Mechanisms in an Entrained Flow Coal Gasifier, Energy & Fuels 24(2) (2010) 1170-1175.
[39] A. Silaen, T. Wang, Investigation of the Coal Gasification Process Under Various Operating Conditions Inside a Two-Stage Entrained Flow Gasifier, Journal of Thermal Science and Engineering Applications 4(2) (2012) 021006-021006-11.
[40] M. Kumar, A.F. Ghoniem, Multiphysics Simulations of Entrained Flow Gasification. Part I: Validating the Nonreacting Flow Solver and the Particle Turbulent Dispersion Model, Energy & Fuels 26(1) (2012) 451-463.
[41] F. Qian, X. Kong, H. Cheng, W. Du, W. Zhong, Development of a Kinetic Model for Industrial Entrained Flow Coal Gasifiers, Industrial & Engineering Chemistry Research 52(5) (2013) 1819-1828.
[42] J. Xu, L. Qiao, Mathematical Modeling of Coal Gasification Processes in a Well-Stirred Reactor: Effects of Devolatilization and Moisture Content, Energy & Fuels 26(9) (2012) 5759-5768.
[43] A. Slezak, J. M. Kuhlman, L. Shadle, J. Spenik, S. Shi, CFD simulation of entrained-flow coal gasification: Coal particle density/sizefraction effects, 2010.
[44] J. Ma, S.E. Zitney, Computational Fluid Dynamic Modeling of Entrained-Flow Gasifiers with Improved Physical and Chemical Submodels, Energy & Fuels 26(12) (2012) 7195-7219.
[45] Y.-P. Chyou, M.-H. Chen, Y.-T. Luan, T. Wang, Investigation of the Gasification Performance of Lignite Feedstock and the Injection Design of a Cross-Type Two-Stage Gasifier, Energy & Fuels 27(6) (2013) 3110-3121.

[46] S. Shabbar, I. Janajreh, Thermodynamic equilibrium analysis of coal gasification using Gibbs energy minimization method, Energy Conversion and Management 65 (2013) 755-763.
[47] L. National Energy Technology, Wabash River Coal Gasification Repowering Project: A DOE Assessment; FINAL, United States, 2002, p. 309Kilobytes.
[48] C.A. Fluent, CFD, version 17.0, ANSYS Inc., Cecil Township, Pennslyvania, USA (2016).
[49] M. Saiful Alam, A.T. Wijayanta, K. Nakaso, J. Fukai, Study on coal gasification with soot formation in two-stage entrained-flow gasifier, International Journal of Energy and Environmental Engineering 6(3) (2015) 255-265.
[50] R.W. Breault, Gasification processes old and new: a basic review of the major technologies, Energies 3(2) (2010) 216-240.
[51] C. He, X. Feng, K.H. Chu, Process modeling and thermodynamic analysis of Lurgi fixed-bed coal gasifier in an SNG plant, Applied Energy 111 (2013) 742-757.
[52] C.K. Westbrook, F.L. Dryer, Simplified Reaction Mechanisms for the Oxidation of Hydrocarbon Fuels in Flames, Combustion Science and Technology 27(1-2) (1981) 31-43.
[53] K. Hou, R. Hughes, The kinetics of methane steam reforming over a Ni/α-Al2O catalyst, Chemical Engineering Journal 82(1) (2001) 311-328.
[54] P. Nakod, CFD Modeling and Validation of Oxy-Fired and Air-Fired Entrained Flow Gasifiers, Int. J. Chem. Phys. Sci 2(6) (2013) 28-40.